On noncommutative dynamic spacetimes

by

©John Bowden

A thesis submitted to the School of Graduate Studies in partial fulfillment of the requirements for the degree of

Masters of Science

Department of Mathematics and Statistics

Memorial University of Newfoundland

May 2014

St. John's Newfoundland

Abstract

Noncommutative gravity is a theory of quantum gravity that presupposes a fuzziness in spatial coordinates. Under the formalism of coherent states, mass is diffused per a gaussian distribution. In this work we begin with a review of existing noncommutative spacetime solutions. We then study the classical Vaidya spacetime with parameters for mass and charge, in the context of noncommutative gravity. The characteristic behaviour of this spacetime is discussed, with particular attention to the moment of formation of the apparent horizon. At this moment, the black hole is extremal, and we discuss the relationship between the mass and charge parameters, and the time and position of the apparent horizon. We follow with a calculation of the stress-energy tensor for a noncommutative Vaidya spacetime, and show violation of the energy conditions. Using a polytropic-like equation of state, we construct a new dynamic spacetime solution that satisfies the dominant energy condition, and encompasses several interpretations via parameter choice.

Acknowledgements

With thanks —

To my supervisor, Dr. Ivan Booth, for his time and expertise. This work has been a long process from start to finish, and Dr. Booth gave many hours to discussion, reviewing, and editing. His help was invaluable to the completion of this work, particularly in understanding the finer points of general relativity, and in working towards precision in this thesis. I am grateful for these many discussions, both the mathematical and the personal.

To my wife, Jane, for listening sympathetically to the many ups and downs of working on this thesis – despite not always understanding what I was talking about. The encouragement went a long way.

Table of Contents

List of Tables

List of Figures

Chapter 1

Introduction

In 1911, the Solvay Conference series on physics and chemistry began, marking a new era in physics, namely quantum physics. In 1927, at the Fifth Solvay Conference, an iconic photograph was taken of the twenty-nine attendees, which included many well-known physicists, including 17 Nobel prize winners. From this photograph, and the people present, it was clear that modern physics was indeed starting something new and exciting. Since that time, atomic theory has become common knowledge, and part of school curricula around the world. Most people can quote Einstein's equation, $E = mc^2$, though with little understanding of its meaning. Nonetheless, it is understood that within this simple equation lies deep meaning.

The misconception is that Einstein earned his Nobel prize for that equation and its associated work. While relativity was mentioned in the award speech, the prize was given for his discovery of the law of the photoelectric effect [2]. Less popularly-known are his descriptions of spacetime, and the equations relating geometry and energy. Since 1915 when he introduced this new understanding of gravity as a result

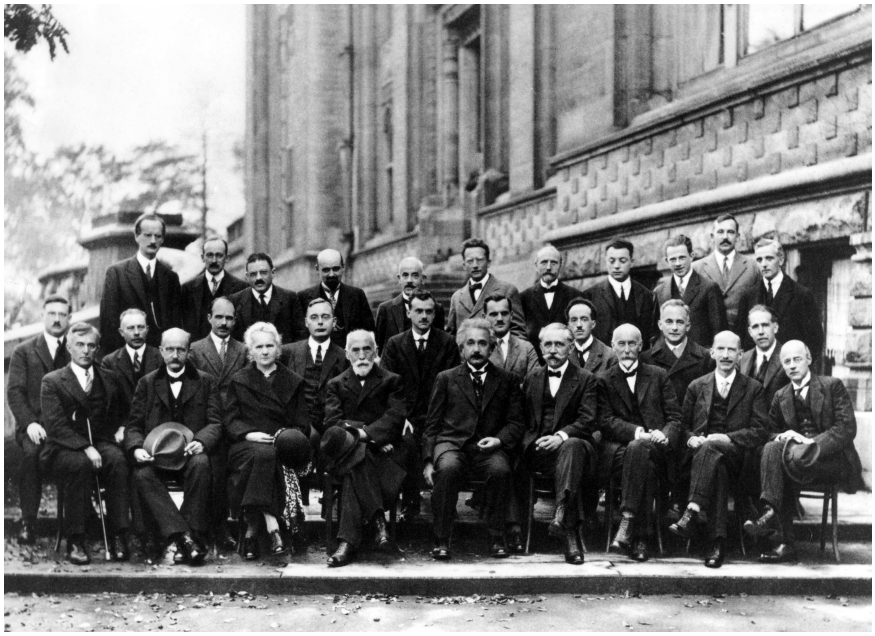

Figure 1.1: Attendees of the Fifth Solvay Conference in 1927. [3]

of geometry [14], work on general relativity has continued alongside research into quantum physics.

A long-standing problem has been the unification of the large with the small. This is popularly-named a "unified theory of everything", that describes both large-scale gravity with small-scale interactions. The challenge is that this theory must smoothly transition between these two very different worlds at appropriate scales. The quantum world is defined by probabilities and uncertainties. None of these appear in a relativistic spacetime theory.

Several models are currently being developed to try and merge these seemingly incompatible theories. Some worthy of note include *loop quantum gravity*, which is one of the most widely accepted [6, 43, 42, 15]; *string theory*, a multi-dimensional theory that describes both gravity and particle interactions; *entropic gravity*, which redefines gravity as an consequence of entropy, and has been met with polarized reactions [49, 1]; *noncommutative gravity*, which integrates Heisenberg's uncertainty principle

into solutions of Einstein's spacetime equations; *amplituhedron theory*, a very recent development in which a fundamental, simplified, geometrical object describes both particle interactions, and possibly gravity.

Loop quantum gravity, LQG, is currently one of the more widely-studied theories of quantum gravity. Ashtekar introduced new variables [6] that transform a gravitational spacetime into a theory that resembles fields of traditional physics. In so doing, it was shown that space is quantized and discrete, and made up of networks of loops. These graphs represent states of a gravitational field.

String theory is also widely-studied, and is promising in that it is able to describe all particle states and interactions. The theory is founded on one-dimensional objects called strings. A single string can present itself as different particles, including gravitons, the purported mediating particle of the gravitational force. In presenting particles in this way, the theory is more fundamental and physically complete. There are several versions of string theory, but they are united in the 11-dimensional M-theory.

Entropic gravity is a new theory proposed by Erik Verlinde [49], and redefines gravity as an *entropic force* and an *emergent phenomenon*. That is, gravity is an observed consequence of the system, and in this particular case, of the tendency of macroscopic bodies to increase their entropy. A difference in entropy between two bodies creates an entropic force. Verlinde argues that gravity is the macroscopic force we observe. This theory was met with quick discussion, well-illustrated by the title of the paper, *Comments on and Comments on Comments on Verlinde's paper "On the Origin of Gravity and the Laws of Newton"* [1].

Most recently, Hamed et al. described a more fundamental structure, the amplituhedron, which may demonstrate space and time to be emergent phenomena [5]. It is

often the case in studies of quantum gravity that unitarity and locality are broken. This new geometrical structure does not require locality and unitarity as a fundamental characteristic, and so greatly simplifies matters. Particle interactions are more easily explained, replacing the long-standing but often cumbersome Feynman diagrams. Further, it may be that this fundamental object is better equipped to describe quantum gravity, demonstrating many ideas to be emergent phenomena.

Noncommutative gravity, the focus of this work, attempts to bridge the quantum world with the large-scale gravity world by including an analogous form of Heisenberg's Uncertainty Principle (*HUP*) in spacetime solutions. In any quantum system, there are many properties that can be measured, including position and momentum (i.e., energy). If any of these is measured with a particular precision, the HUP states that there is a limit on the precision with which any other property can be measured. This is not a restriction on one's ability to measure at a given precision but a natural limit. As a consequence, a small-scale model of gravity cannot state with certainty the location of any point-mass. There is a natural limit to the precision of spacetime coordinates. This translates into a "fuzziness" of coordinates which then modifies spacetime solutions.

The aim of this work is to investigate this "fuzziness" as part of black-hole formation in a dynamic model, that incorporates both mass and charge. We begin in Chapter 2 with a brief discussion of foundational concepts, including basic spacetime definitions and well-known classical solutions to Einstein's equations. This is followed in Chapter 3 by an overview of existing research and results in noncommutative spacetime. Finally, we present our own work in Chapter 4. We discuss a generalized, noncommutative, and dynamic spacetime solution that encompasses all of the classical parameters. We calculate densities and pressures for the generalized spacetime, and examine them in light of the energy conditions. We investigate extremality for

a noncommutative Reissner-Nordström black hole, and find a "maximally extremal" black hole. Finally, in Chapter 5 we derive a noncommutative solution that satisfies the dominant energy condition and encompasses multiple interpretations.

Where applicable, we use geometrized units with $G = c = 1$. Greek indices $\alpha, \beta, ...$ are used in four-dimensional cases, while roman indices $a, b, ...$ are used in three-dimensional cases. The spacetime signature used will be $(-+++)$. Coordinates will be either spherical (t, r, ϑ, ϕ), or null ingoing Eddington-Finkelstein-type (v, r, ϑ, ϕ). Mathematica was used to create all figures, and to carry out any non-trivial calculations. The *Riemannian Geometry & Tensor Calculus* package was used for tensor calculations.[1]

[1] http://www.inp.demokritos.gr/ sbonano/RGTC/

Chapter 2

Spacetime

The majority of what follows can be found in many introductory and semi-advanced texts, such as those by Wald [50], Hartle [22], Poisson [40], and Griffiths and Podolský [19]. Unless otherwise noted, or requiring more specific referencing, further details can be found in these sources.

2.1 Einstein's equations

The study of four-dimensional spacetime, spacetime curvature, and subsequently black holes, began in earnest with the advent of Einstein's field equations. Through this theory, there is a relation between the matter and energy of a spacetime, represented by the *stress-energy tensor* $T_{\alpha\beta}$, and the *Einstein curvature tensor* $G_{\alpha\beta}$, related by the the Einstein field equations

$$G_{\alpha\beta} = \frac{8\pi G}{c^4} T_{\alpha\beta}. \tag{2.1}$$

The *normalized* Einstein field equations read

$$G_{\alpha\beta} = 8\pi\, T_{\alpha\beta}. \tag{2.2}$$

The Einstein tensor $G_{\alpha\beta}$ is shorthand for a specific combination of objects: the *Ricci curvature tensor* $R_{\alpha\beta}$, the *Ricci scalar curvature* R, and the spacetime metric $g_{\alpha\beta}$:

$$R_{\alpha\beta} - \frac{1}{2} g_{\alpha\beta} R = \frac{8\pi G}{c^4}\, T_{\alpha\beta} \tag{2.3}$$

The Ricci tensor and scalar are contractions of the Riemann tensor $R^{\mu}{}_{\nu\alpha\beta}$, which may be defined as the tensor satisfying

$$V^{\mu}{}_{;\alpha\beta} - V^{\mu}{}_{;\beta\alpha} = -R^{\mu}{}_{\nu\alpha\beta} V^{\nu}, \tag{2.4}$$

for any vector field V^{μ}.

Alternatively, the Riemann tensor may be defined as the factor describing acceleration of geodesic deviation. In an arbitrarily-curved manifold, one can describe the deviation of two geodesics; that is, how quickly they separate from each other. Consider a family of geodesics, $x^{\alpha}(s,t)$, where s labels each geodesic, and t is an affine parameter along each geodesic. For fixed s, $u^{\alpha} = \frac{\partial x^{\alpha}}{\partial t}$ is a vector field tangent to the geodesics. As well, for fixed t, $\xi^{\alpha} = \frac{\partial x^{\alpha}}{\partial s}$ is a vector field tangent to curves parameterized by s, which are generally not geodesics themselves. This vector ξ^{α} is a deviation vector, describing the separation of neighbouring geodesics. The acceleration of this deviation can be derived as [40]

$$\frac{D^2 \xi^{\alpha}}{dt^2} = -R^{\alpha}{}_{\beta\gamma\delta} u^{\beta} \xi^{\gamma} u^{\delta} \tag{2.5}$$

The Riemann tensor has 20 independent components, and is anti-symmetric in the first two indices, and the last two indices.

The Ricci tensor is a contraction of the Riemann tensor, over the deviation indices in Equation 2.5, α and γ:

$$R_{\beta\delta} = R^{\mu}{}_{\beta\mu\delta}. \tag{2.6}$$

In a vacuum spacetime, $R_{\alpha\beta} = 0$. The Ricci scalar is again a contraction,

$$R = R_{\alpha\beta}R^{\alpha\beta}. \tag{2.7}$$

2.2 Causality

The notion of causality is essential to the definition of 4-dimensional spacetime. A *worldline* is the path through a 4-dimensional spacetime that an observer follows. A worldline can be *timelike*, *spacelike* or *null*. Observers with a speed less than the speed of light ($c = 1$) move on timelike worldlines such that $ds^2 < 0$, where ds represents an infinitesimal length segment along the worldline curve. Light rays have null worldlines, $ds^2 = 0$. Spacelike curves can only be travelled at speeds greater than c: $ds^2 > 0$; hypothesized particles such as tachyons would travel along these types of curves. For a point in space, null (light) rays emanating from that point trace out a *light cone* which is the region of space through which a timelike observer may move in his future. We must stop at this point and discuss precisely what we mean by *future*. This may seem pedantic, but many discussions that may follow from these ideas require rigour. Notions of what "flat" space means, for example, is quite involved; even the definition of a black hole as a global feature of a spacetime requires precision in these ideas.

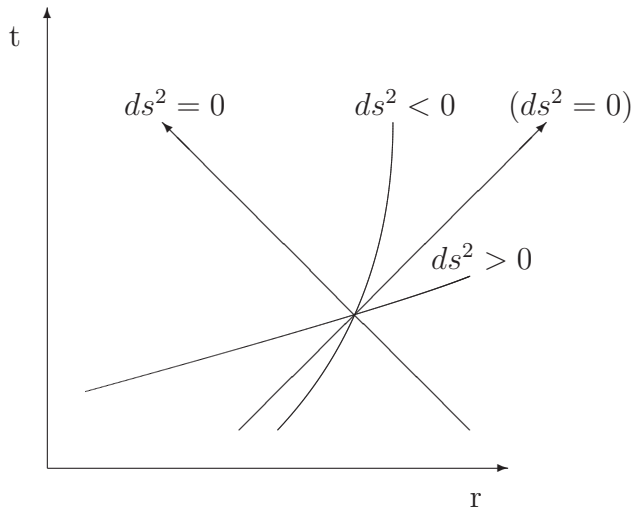

Figure 2.1: The three types of worldlines

A spacetime extends to spatial and timelike infinity, and it is assumed that worldlines may continue "forever", unless they reach a singularity, for example. The issue at hand is where they end up; while limits are calculable, it is preferable to have a better way of talking about these "places".

By applying a conformal transformation ([50; Ch 11]), a spacetime (more specifically, the manifold) can have points added-in, where these points represent the infinities. These are, for Minkowski space,

- *Past (Future) null infinity* All null rays begin (end) here, labelled $\mathscr{I}^-$ ($\mathscr{I}^+$).
- *Spacelike infinity* All spacelike curves begin and end here, labelled i^0.
- *Past (Future) timelike infinity* All timelike curves begin (end) here, labelled i^- (i^+).

In Figure 2.2, a Penrose diagram is shown for the Schwarzschild black hole, where there is also the point $r = 0$, which is the singularity. While some future-oriented

null worldlines may arrive at $r = 0$, none that arrive at $\mathscr{I}^+$ have $r = 0$ in their past. This is in fact a definition of a black hole: that region from which no null causal curves arrive at $\mathscr{I}^+$ as $t \to \infty$. (This is an unfortunately cumbersome definition, as it requires omniscience of the spacetime for all time, past and future.)

Euclidean space is called "flat", and the most basic 4-dimensional spacetime, Minkowski space, is also flat. Other spacetimes such as (anti-)deSitter are not necessarily flat, and in the presence of matter, are certainly not so. These curved spacetimes however do often become flat at spacelike infinity. They are called asymptotically flat, and while intuitively simple, the rigorous definition of this character is quite detailed [50; p.276].

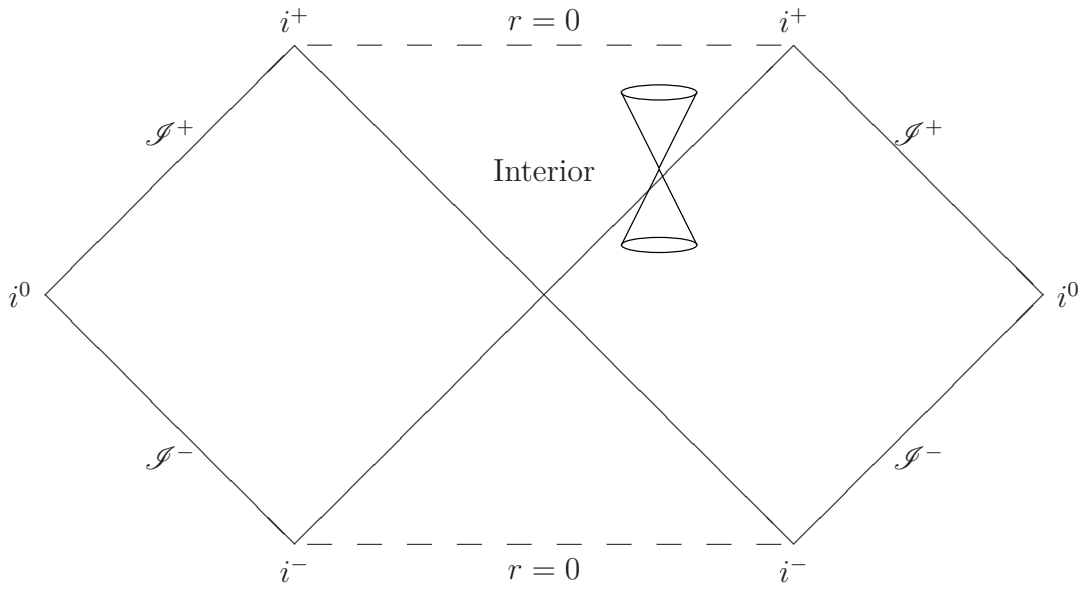

Figure 2.2: Penrose diagram for the Schwarzschild black hole solution

2.3 Black hole definitions

2.3.1 By Causality

A black hole is a *global* feature of the spacetime; there is no purely local definition of a black hole, though quasi-local models do exist. One requires a complete knowledge of the spacetime so that the "black" region of the spacetime can be identified. In effect, one must observe the behaviour of all null rays in the spacetime for all of time. The black hole is then that region of space from which all null rays do not reach future null infinity. That region is causally separated from future null infinity; any null (and therefore, timelike) curve within that region cannot escape to the outside region.

.

As shown in Figure 2.3, lightcones are drawn for various points inside and outside the black hole. Due to the curvature of the spacetime, the cones begin tipping towards the horizon as they approach it. Timelike worldlines lie inside those cones, and must travel faster to escape the black hole. The edge of the cone is traced by null rays, which cannot escape once the cone is at the horizon.

2.3.2 Trapped surfaces

On a given spacelike 2-surface, define two future-directed null normals, ℓ^a (outward) and n^a (inward). These two vectors generate null fields, with expansions as follows, where $\tilde{q}^{ab}$ is the intrinsic metric on the 2-surface.

$$\theta_{(\ell)} = \tilde{q}^{ab}\nabla_a \ell_b \tag{2.8}$$

$$\theta_{(n)} = \tilde{q}^{ab}\nabla_a n_b \tag{2.9}$$

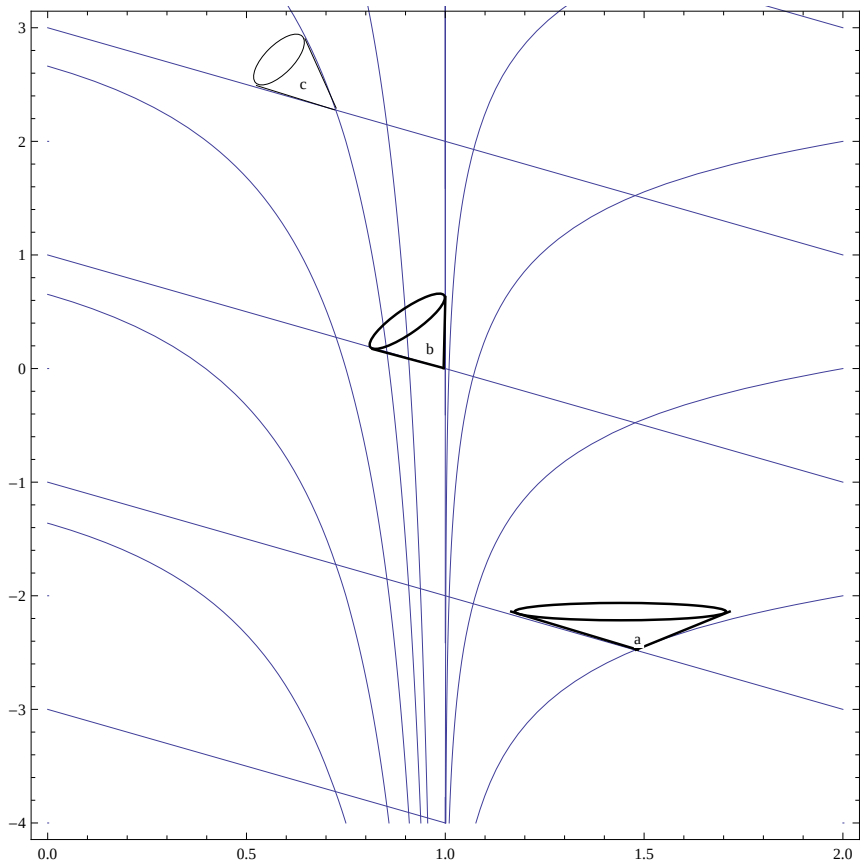

Figure 2.3: Schwarzschild spacetime diagram in ingoing null coordinates. (a - outside the event horizon; b - at the event horizon; c - inside the event horizon)

Consider a series of spherical shells of various radii centred at the origin $r = 0$. The expansions would be $\theta_{(n)} < 0$ and $\theta_{(\ell)} > 0$: the inward vector field converges towards the centre, and the outward vector field diverges. However, in a spacetime with a black hole, this is not always the case. As shown in Figure 2.3, null rays (which would be tangent to the null vector fields ℓ^a and n^a) cannot escape the horizon. Outward light rays at the horizon remain parallel to it; in the interior, both inward- and outward-light-rays converge to the centre. The expansions then must change accordingly. Any sphere of constant r has a negative inward expansion, $\theta_{(n)} < 0$. The sign of the outward expansion then changes on either side of the black hole horizon. Outside the horizon, $\theta_{(\ell)} > 0$, indicating that outward-pointing light rays diverge (ie., escape the black hole). At the horizon, $\theta_{(\ell)} = 0$, and this sphere is called a *marginally trapped surface*. Spheres within the black hole are called *fully trapped surfaces*, and have $\theta_{(\ell)} < 0$, in addition to the expected $\theta_{(n)} < 0$.

2.4 Spacetime Solutions

2.4.1 Minkowski spacetime

The most basic of spacetimes is the Minkowski spacetime,

$$\eta_{\alpha\beta} = \begin{pmatrix} -1 & 0 & 0 & 0 \\ 0 & 1 & 0 & 0 \\ 0 & 0 & 1 & 0 \\ 0 & 0 & 0 & 1 \end{pmatrix}. \tag{2.10}$$

This spacetime is a four-dimensional pseudo-Riemannian spacetime. It is not purely Riemannian, since the signature is negative in the first coordinate, $(-+++)$. It is a vacuum solution, and so from the Einstein equations we have $T_{\alpha\beta} = R_{\alpha\beta} = 0$. The fact that $T_{\alpha\beta} = 0$ tells us there is no matter; $R_{\alpha\beta} = 0$ tells us the space is Ricci flat.

The Minkowski spacetime is diffeomorphic to $\mathbb{R}_t \times \mathbb{R}^3$, where we have labelled $\mathbb{R}_t$ as the time dimension. For a given subspace of constant-t the metric is a classical Euclidean metric, with a line-element in Cartesian coordinates

$$ds^2 = dx^2 + dy^2 + dz^2 \geq 0 \tag{2.11}$$

For a timelike-curve (constant spatial coordinates x^α, $\alpha = 1, 2, 3$), the line element is simply

$$ds^2 = -dt^2 \leq 0 \tag{2.12}$$

This was discussed previously; again, this characterizes our classification of worldlines as spacelike or timelike.

In what follows, the spacetimes that we will study are *asymptotically flat*. In the same way that a Newtonian gravitational field vanishes at large distance, an asymptotically flat spacetime has localized curvature, and becomes Minkowskian at large distance from that locality.

2.4.2 Spherically-symmetric spacetimes

A particular class of spacetimes are those that are *spherically symmetric*: the metric is has an SO(3) symmetry and so is invariant under all rotations. As such, any 2-sphere

is characterized by its area. The function

$$r = \sqrt{A/4\pi} \tag{2.13}$$

defines the line-element of the 2-sphere as

$$ds^2 = r^2 \left(d\vartheta^2 + \sin^2 \vartheta d\phi^2 \right). \tag{2.14}$$

The function r is often called the "radial" distance, measured from some centre. In Euclidean space, this is an appropriate description; for any other curved space, this function may not measure such a distance. Nonetheless, the nomenclature remains.

For a 4-dimensional spacetime, in spherical coordinates $x^\mu = (t, r, \vartheta, \phi)$, a spherically-symmetric spacetime can be written with a line-element of

$$ds^2 = -\mathrm{e}^{\psi(r)} dt^2 + \mathrm{e}^{\chi(r)} dr^2 + r^2 d\Omega^2 \tag{2.15}$$

where $d\Omega^2 = (d\vartheta^2 + \sin^2 \vartheta d\phi^2)$. This is a *static* line-element: it is invariant under time translations $t \to t +$ constant, as well as time reflections $t \to -t$. A spacetime invariant under time translations is called *stationary*, and possesses a timelike Killing vector field. A rotating spacetime, for example, is stationary but not static: if $t \to -t$ its direction of rotation reverses.

A stationary but nonstatic spacetime that uses the Killing vector parameter as a coordinate must have cross-terms $dx^\mu dx^\nu$, $\mu \neq \nu$ [50; p.119]. The Vaidya solution is a spherically-symmetric solution with cross-terms, but it is a non-stationary solution as it does not have the appropriate Killing vector.

2.4.2.1 The Schwarzschild solution

The Schwarzschild solution to Einstein's spacetime equations is a spherically-symmetric, static (ie. time-independent) spacetime which contains a black hole. The Schwarzschild metric is defined as Equation 2.15 with $e^{\psi(r)} = (1 - 2M/r)$, $e^{\chi(r)} = e^{-\psi(r)}$, where M is the mass of the black hole.

The line element then reads,

$$ds^2 = -\left(1 - \frac{2M}{r}\right) dt^2 + \left(1 - \frac{2M}{r}\right)^{-1} dr^2 + r^2 d\Omega^2. \tag{2.16}$$

The Schwarzschild solution is independent of time (coordinate t), and is static. We will later see that the Vaidya solution modifies this, and the spacetime becomes dynamical in that the mass becomes a function of time. This has further consequences for the horizon of the black hole, which requires differentiating between the *apparent horizon*, and the *event horizon*.

The event horizon in the Schwarzschild solution occurs when $(1 - 2M/r)^{-1}$ becomes singular, that is when $r = 2M$. For $r > 2M$, the r-coordinate is spacelike ($ds^2 = f^{-1}dr^2 > 0$), and the t-coordinate is timelike ($ds^2 = -f dt^2 < 0$). When the event horizon is crossed, this signature changes; r becomes timelike, and t becomes spacelike.

The Schwarzschild spacetime solution has two important objects: a singularity found at $r = 0$ and a horizon at $r = 2M$. The singularity $r = 0$ is a global object, independent of the choice of coordinate systems. The other locus, the Schwarzschild horizon $r = 2M$, is coordinate-system-dependent. We can introduce other coordinate systems that remove this singularity, but also add other benefits, in that these systems make some of the properties clearer.

The first coordinate system we will examine is a null-coordinate system, so that the coordinates (t, r) are replaced by coordinates (v, r). In this coordinate system, v is a null coordinate, so that curves of constant-v are null rays. This is the *Eddington-Finkelstein* coordinate system. The derivation is as follows.

We have a spherically-symmetric metric

$$ds^2 = -f(t,r)dt^2 + f(t,r)^{-1}dr^2 + r^2 d\Omega^2 \tag{2.17}$$

where at $r = r_h$, f becomes singular. We want to remove $f(t,r)^{-1}$, by defining a new coordinate r^*, called the *tortoise coordinate*, in such a way that

$$dr^* = \left(1 - \frac{2M}{r}\right)^{-1} dr \tag{2.18}$$

Integrating, we find

$$r^* = r + 2GM \ln\left|\frac{r}{2M} - 1\right| \tag{2.19}$$

Define the coordinate $v = t + r^*$. This creates a null coordinate, so that curves of constant-v are null geodesics. The metric in (v, r) Eddington-Finkelstein coordinates (with r^* relabelled as r) is

$$ds^2 = -\left(1 - \frac{2M}{r}\right) dv^2 + 2dvdr + r^2 d\Omega^2 \tag{2.20}$$

The coordinate v is an *ingoing* coordinate, so that curves of constant-v are ingoing towards $r = 0$. Likewise, one can define an *outgoing* coordinate $u = t - r^*$, where curves of constant-u are null rays in the direction of increasing r. The outgoing metric has the term $2dvdr$ replaced by $-2dudr$.

Other null curves satisfy

$$\frac{dv}{dr} = \left(1 - \frac{2M}{r}\right) \tag{2.21}$$

It is immediate from the metric that $r = 0$ is still a singularity, but the singularity at $r = 2M$ has been removed.

For future discussion, we will need a pair of null vectors that are normal to a cross-section of the horizon. Here we consider the more general case of the null normals to any surface of constant v and r. The line-element reads more generically as

$$ds^2 = -f(v,r)dv^2 + 2\epsilon dvdr + r^2 d\vartheta^2 + r^2 \sin^2\vartheta d\phi^2 \tag{2.22}$$

Note that $\epsilon = \pm 1$, so that the sign of ϵ determines whether v is an ingoing coordinate ($\epsilon = +1$) or an outgoing coordinate ($\epsilon = -1$).

Since we are dealing with a spherically-symmetric spacetime, any null normal vector will be independent of ϑ and ϕ, and will be tangent to null curves, such that $ds^2 = 0$. In particular,

$$ds^2 = -f(v,r)dv^2 + 2dvdr = 0 \tag{2.23}$$

These null curves satisfy either $v = 0$, or $dr = \frac{f(v,r)}{2}dv$. We also require that the two vectors be cross-normalized,

$$n^\alpha \ell_\alpha = -1 \tag{2.24}$$

Ingoing and outgoing null vectors that satisfy these requirements are

$$n^\alpha = \left(-1, \frac{f}{2}, 0, 0\right) \tag{2.25}$$

$$\ell^\alpha = (0, 1, 0, 0) \tag{2.26}$$

2.4.2.2 Reissner-Nordström

The Reissner-Nordström metric is a spherically-symmetric spacetime, similar to the Schwarzschild metric, but with the addition of an electric charge, Q. The metric function $f(r)$ read as

$$f(r) = 1 - \frac{2M}{r} + \frac{Q^2}{r^2}. \tag{2.27}$$

This spacetime is also degenerate at $r = 0$, and admits a black hole of mass M, with horizons at $r = M \pm \sqrt{M^2 - Q^2}$. There are now two horizons, $r_+ = M + \sqrt{M^2 - Q^2}$ and $r_- = M - \sqrt{M^2 - Q^2}$, so that $0 < r_- < M < r_+ < 2M$. In the case $Q = 0$, the horizons become $r_+ = 2M$ and $r_- = 0$, which is the Schwarzschild solution. In the case $M = Q$, there is a single horizon, $r_H = r_+ = r_- = M$. This is called an *extremal black hole*.

The signature of the r-coordinate changes at these two horizons, and is another interesting feature of this spacetime. In the Schwarzschild solution, the singularity at $r = 0$ is a spacelike surface. For $r > 2M$, surfaces of constant-r are timelike; for $r < 2M$, the sign of $1 - 2M/r$ changes, and surfaces of constant-r are now spacelike. In the Reissner-Nordström solution, there are two horizons (three regions) to consider. The sign of $f(r)$ changes at each horizon. Surfaces of constant-r are timelike for $r > r_+$, spacelike for $r_+ > r > r_-$, and timelike for $r_- > r$. That is, $r = 0$ is a timelike surface, and so can be avoided by an infalling observer. Because r is a spacelike coordinate for $r < r_-$, an observer can move towards, or away from it. Similarly, for an observer who has already crossed r_+, there is no possibility of avoiding r_-: r decreases necessarily (it is a *timelike* coordinate), and so the observer must cross it. Can the observer, being able to move away from $r = 0$ escape out of the black hole? They may indeed cross over $r = r_-$ to an outer region, but this is not so straight-forward. Once they do, they are in fact in a different 'universe'. Again, r is a timelike coordinate, and

they are forced back into another region where $r < r_-$. Despite the change in sign of f, any observer, signal, or information is forever trapped inside $r = r_+$, regardless of the universe. See in particular the Penrose diagram in Fig.9.7 in [19].

2.4.2.3 The Vaidya solution

A very intuitive modification to the Schwarzschild spacetime in order to make it dynamic is to modify the mass function to be time-dependent. Such a modification does indeed make it a solution to Einstein's equation. There are requirements however, on the form of the mass equation so that the spacetime does not contradict the energy conditions, which we will discuss below.

The corresponding Vaidya metric is then

$$g_{\alpha\beta} = \begin{pmatrix} -\left(1 - \frac{2m(v)}{r}\right) & \epsilon & 0 & 0 \\ \epsilon & 0 & 0 & 0 \\ 0 & 0 & r^2 & 0 \\ 0 & 0 & 0 & r^2 \sin^2(\vartheta) \end{pmatrix}. \tag{2.28}$$

The function $m(v)$ can be taken as increasing or decreasing, depending on the model. The choice of coordinate system also determines the type of hole. Using ingoing coordinates, an increasing mass indicates a black hole accreting material, while a decreasing mass function with outgoing coordinates is often used to represent a (Hawking) radiative black hole. Outgoing coordinates describe a white hole. It is important to note that while the Schwarzschild solution can be interpreted in both ingoing and

outgoing Eddington-Finkelstein coordinates, the Vaidya solution cannot. The null coordinates in the Vaidya solution are indeed analogous to the ingoing Eddington-Finkelstein coordinates in a Schwarzschild solution, but are not identical. One cannot simply "switch" to outgoing coordinates, and maintain the spacetime behaviour. The Vaidya solution has a mass function and a radial tortoise coordinate that are both dependent on the ingoing v-coordinate. Changing to an outgoing u-coordinate would fundamentally change these other quantities, which in turn has significant effects on the behaviour of the spacetime. The matter we will consider can be interpreted as a *null dust*: null meaning that it in-falls along null curves, and dust meaning that it is pressureless.

The dynamic nature of the Vaidya solution makes the behaviour of the horizon more interesting. We are able to say more about the development of this horizon. For a horizon that settles down into equilibrium as $v \to \infty$, $m(v) \to M$, and $r_h \to 2M$. The horizon found at $r = 2m(v)$ is the *apparent horizon*, but it is not the *event horizon*. Suppose an observer is close to $r = 0$ before the apparent horizon forms; can they still escape? In fact, depending on the time at which they leave $r = 0$ and try to escape, they may or may not make it.

Consider the following Figure 2.4.2.3, showing the horizon as m grows. This is the apparent horizon. Consider a light ray that finishes at late time at the horizon. Any observer would move with less speed, and would still be trapped if they were within the light cone traced by that ray. We take a geodesic at late time v, and integrate it backwards towards $r = 0$. We see then that this light ray creates another horizon, behind which no observer can escape, even if they attempted to do so before the formation of the black hole. This is the *event horizon*. In a static solution, like Schwarzschild, the apparent and event horizons are the same.

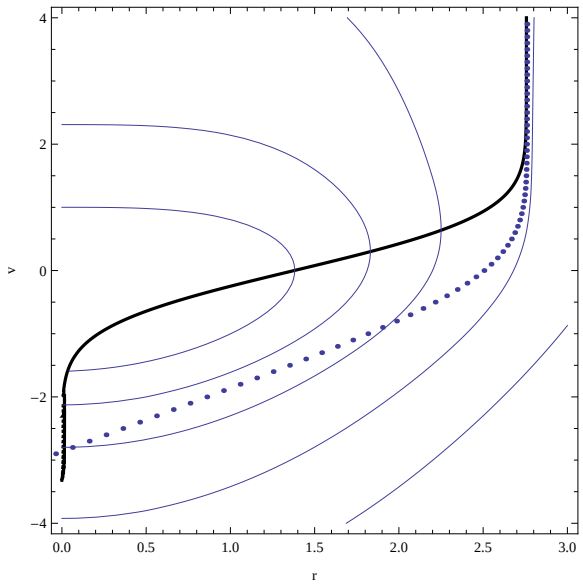

Figure 2.4: Horizons of a Vaidya solution with $m(v) = \frac{m_f}{2}\left(1 + \mathcal{E}\left(v\right)\right)$.(The thick line is the apparent horizon; the dotted line is the event horizon; the thin lines are outgoing null rays)

Chapter 3

Literature review of noncommutative gravity

3.1 Motivation

For a number of years, there has been a desire to unite different-scale physics: the large-scale gravitational regime with the small-scale quantum regime. It is assumed that at a quantum scale, there should be an adapted theory of gravity. Perhaps the most serious problem is that there exists no observational results of quantum gravity to motivate any particular theoretical direction. The focus of this work is the noncommutative model.

Noncommutativity is a characteristic that already exists in quantum physics. In a phase space, operators do not generally commute due to the Heisenberg Uncertainty Principle. This principle states that if a particle is measured with position x and momentum p, there is a lower limit on the precision of these measurements of $\Delta x \Delta p \geq$

$\hbar$. Note that the limit is not a technological one, but phenomenological: the quantum world *prevents* arbitrarily-precise, simultaneous measurements of multiple quantities.

Two thought experiments suggest the noncommutativity of quantum gravity:

Example 3.1.1. Noncommutative thought experiment I [13]

Consider a particle for which we measure its position x with increasing precision. As a result, the momentum, p, of the particle is measured with decreasing precision. By the Heisenberg Uncertainty Principle, we can force the precision Δp to be divergent by increasing our precision of measurement of the position. This effective increase in momentum is equivalent to an increase in energy, creating an uncertainty in the curvature at the location of measurement. This uncertainty of curvature increases with the precision of measurement of position. We create a paradox thusly: an increase in precision of measurement of position creates a sufficiently divergent curvature, which induces a region about the particle from which signals cannot escape, preventing the arbitrarily precise measurement of position.

Example 3.1.2. Noncommutative thought experiment II [20]

Assume a flat spacetime with a single electron for which we want to measure position. A photon with energy E is sent in the direction of this particle; the wavelength of this photon is $\lambda \approx hcE^{-1}$. This is the maximum precision with which the position of our photon can be determined. This implies that this is also the precision with which we can measure the position of the electron.

Suppose now that we also want to measure the position of the electron in the direction transverse to the motion of our photon. Our photon also has a Schwarzschild radius of $r_S \approx GEc^{-4}$. No information from inside this radius can be extracted. At best, we can say whether the electron is inside or outside this radius. The radius r_S increases with E, unlike λ which decreases with E. These measurements contradict each other.

Their product is

$$\lambda r_S = (hcE^{-1})(GEc^{-4}) = hGc^{-3} = \ell_P^2 \tag{3.1}$$

The smallest perceivable area is then ℓ_P^2.

To introduce noncommutativity on a manifold, there have been two main approaches. The first was to mimic operators on a phase space by viewing spacetime as an algebra of functions with a modified, noncommutative, $\star$-product. The second is to introduce fuzziness in the metric functions, referred to as *coherent states*. In either case, coordinates x^μ are considered noncommuting when

$$[x^\mu, x^\nu] = \theta^{\mu\nu} \tag{3.2}$$

for a constant skew-symmetric matrix $\theta^{\mu\nu}$.

3.1.1 Algebra with $\star$-product

One of the first approaches to noncommutative geometry was inspired by the field of quantum mechanics, where measures are operators on a phase space. An accessible introduction to this is found in Chaichian et al. [11], and we briefly reproduce the foundation here.

Let U be a region in $\mathbb{R}^2$, with coordinates (t_1, t_2). Let $\bar{h} \in \mathbb{R}$, and denote $\mathbb{R}[[\bar{h}]]$ the ring of formal power series of $\bar{h}$. That is, $\mathbb{R}[[\bar{h}]]$ is the set of infinite polynomials of $\bar{h}$ with an addition and a multiplication.

Next $\mathbb{R}[[\bar{h}]]$ is extended to a module over itself. A module is akin to a vector space over a field; here, it is over a ring. Let $\mathcal{A}$ be the set of formal power series in $\bar{h}$, but

with coefficients that are smooth real functions over U. Elements of $\mathcal{A}$ are written $\sum_{i\geq 0} f_i \bar{h}^i$.

For any two functions f and g on U, denote fg as the point-wise product of f and g. Define also a noncommutative star product, $f \star g$, as the *Moyal product* [31],

$$f \star g = \lim_{t' \to t} \exp\left[\bar{h}\left(\frac{\partial}{\partial t_1}\frac{\partial}{\partial t'_2} - \frac{\partial}{\partial t_2}\frac{\partial}{\partial t'_1}\right)\right] f(t)g(t'). \tag{3.3}$$

It is assumed that $\exp(\cdot)$ is a power series in the derivative operator above. The noncommutativity is apparent when written in the form [52],

$$\exp\left[\bar{h}\left(\frac{\partial}{\partial t_1}\frac{\partial}{\partial t'_2} - \frac{\partial}{\partial t_2}\frac{\partial}{\partial t'_1}\right)\right] = \exp\left[\bar{h}\left(\sum_{i,j}\theta_{ij}\frac{\partial}{\partial t_i}\frac{\partial}{\partial t'_j}\right)\right] \tag{3.4}$$

For elements in $\mathcal{A}$, which are power series of functions, this $\star$-product is extended and defined as

$$\left(\sum f_i \bar{h}^i\right) \star \left(\sum g_j \bar{h}^j\right) = \sum \left(f_i \star g_j\right) \bar{h}^{i+j} \tag{3.5}$$

A metric on $\mathcal{A}$ is created as follows. Let $\mathcal{A}^3 = \mathcal{A} \oplus \mathcal{A} \oplus \mathcal{A}$. Define a *dot product* "$\bullet$" on $\mathcal{A}^3 \otimes_{\mathbb{R}[[\bar{h}]]} \mathcal{A}^3$ as

$$\mathcal{A}^3 \otimes_{\mathbb{R}[[\bar{h}]]} \mathcal{A}^3 \to \mathcal{A}, (a,b,c) \otimes (f,g,h) \mapsto a \star f + b \star g + c \star h \tag{3.6}$$

for any $(a,b,c),(f,g,h) \in \mathcal{A}^3$. Then for any $X = (X^1, X^2, X^3) \in \mathcal{A}^3$ (indices,not powers), define $\partial_i X = (\partial_i X^1, \partial_i X^2, \partial_i X^3)$. The metric g_{ij} on $\mathcal{A}$ is defined as

$$g_{ij} = \partial_i X \bullet \partial_j X \tag{3.7}$$

The metric g_{ij} has inverse g^{ij} with the expected property

$$g_{ij} \star g^{jk} = \delta_i{}^k \tag{3.8}$$

Chaichian et al. in [11] continue the construction of noncommutative Riemannian geometry with the development of a connection on $\mathcal{A}$, as well as curvature objects. This construction began with a two-dimensional deformation of $\mathbb{R}^2$. This can be extended to arbitrarily high dimensions [11, 52].

A noncommutative Schwarzschild solution under this formalism is now presented, as an embedding in a 6-dimensional space. The noncommutative metric reads [52]

$$\begin{aligned}
g_{00} &= -\left(1 - \frac{2M}{r}\right) \\
g_{01} &= g_{10} = g_{02} = g_{20} = g_{03} = g_{30} = 0 \\
g_{11} &= \left(1 - \frac{2M}{r}\right)^{-1} \left[1 + \left(1 - \frac{2M}{r}\right)(\sin^2\vartheta - \cos^2\vartheta)\sinh^2\bar{h}\right] \\
g_{12} &= g_{21} = 2r\sin\vartheta\cos\vartheta\sinh^2\bar{h} \\
g_{13} &= -g_{31} = -2r\sin\vartheta\cos\vartheta\sinh\bar{h}\cosh\bar{h} \\
g_{22} &= r^2[1 - (\sin^2\vartheta - \cos^2\vartheta)\sinh^2\bar{h}] \\
g_{23} &= -g_{32} = r^2(\sin^2\vartheta - \cos^2\vartheta)\sinh\bar{h}\cosh\bar{h} \\
g_{33} &= r^2[\sin^2\vartheta + (\sin^2\vartheta - \cos^2\vartheta)\sinh^2\bar{h}]
\end{aligned} \tag{3.9}$$

The deformed Schwarzschild still retains a horizon at $r = 2M$, temperature of $T = 1/4M$, and entropy $S_{bh} = 4\pi M^2$. However, the area of the black hole has $\bar{h}$-corrections,

$$A = 16\pi M^2\left(1 - \frac{\bar{h}^2}{6} + \mathcal{O}(\bar{h}^4)\right). \tag{3.10}$$

There are however, issues with this approach [34]. At the level of free fields, the $\star$-product-deformed theory is identical to the original theory. The theory does not satisfy unitarity [18]: the sum of quantum probabilities for a given event do not add up to 1. Lastly, the theory does not cure UV divergences. That is, there are effects at a given scale from objects with energies at a different energy scale. It is the perturbative nature of the parameter $\bar{h}$ at the heart of these issues.

Various attempts have been made at creating a noncommutative Schwarzschild solution, similar to what was presented above [34, 12, 25, 24]. Among these approaches, there are still unwanted powers of $1/r$ that persist.

3.1.2 Coherent states

The problems presented by the $\star$-product approach have been solved by the consideration of *coherent states* [17]. We present here two pieces of motivating work: a development of a quantum field theory that encodes noncommutativity as a gaussian distribution, as well as a quantum system that replaces the usual dirac position operator with a gaussian distribution.

The following construction of the noncommutative quantum field theory is by Smailagic and Spallucci [46].

The noncommutative spatial plane has coordinates $\mathbf{X^i}$, momenta $\mathbf{P_j}$, $i, j = 1, 2$ and commuting relations

$$\begin{aligned} \left[\mathbf{X^i}, \mathbf{X^j}\right] &= \mathrm{i}\theta\epsilon_{ij} \\ \left[\mathbf{X^i}, \mathbf{P_j}\right] &= \mathrm{i}\delta^i{}_j \\ \left[\mathbf{P_i}, \mathbf{P_j}\right] &= 0. \end{aligned} \tag{3.11}$$

It is immediate that the plane is now "blurry", and the position operators $\mathbf{X_1}$ and $\mathbf{X_2}$ do not share any common eigenstates. Define new operators $\mathbf{Z}$ and $\mathbf{Z}^\dagger$ as

$$\begin{aligned} \mathbf{Z} &\equiv \frac{1}{\sqrt{2}}\left(\mathbf{X^1} + \mathrm{i}\mathbf{X^2}\right) \\ \mathbf{Z}^\dagger &\equiv \frac{1}{\sqrt{2}}\left(\mathbf{X^1} - \mathrm{i}\mathbf{X^2}\right). \end{aligned} \tag{3.12}$$

which satisfy

$$\left[\mathbf{Z}, \mathbf{Z}^\dagger\right] = \theta, \tag{3.13}$$

This last equation is the commutation relation for the creation and annihilation operators. In a quantum field theory, these operators create and annihilate particles in a given state. There then exist *coherent states* (i.e., eigenstates) $|Z\rangle$, of the annihilation operator, satisfying

$$\begin{aligned} \mathbf{Z}|Z\rangle &= z|Z\rangle \\ \langle Z|\mathbf{Z}^\dagger &= \langle Z|\bar{z} \end{aligned} \tag{3.14}$$

for complex eigenvalues z and $\bar{z}$.

For any operator $F(\mathbf{X^1}, \mathbf{X^2})$ which is a function of $\mathbf{X^1}$ and $\mathbf{X^2}$, the aim is to find the mean expectation value $F(z)$,

$$F(z) = \langle z|F(\mathbf{X^1}, \mathbf{X^2})|z\rangle. \tag{3.15}$$

Using a noncommutative form of the Fourier transform,

$$F(z) = \int \frac{d^2p}{2\pi} f(p)\langle z|\exp\left(\mathrm{i}p_j\mathbf{X^j}\right)|z\rangle \tag{3.16}$$

where $\langle z|\exp(\mathrm{i}p_j\mathbf{X^j})|z\rangle$ is the mean expectation value of a plane wave. Choosing $f(p) =$ constant gives the maximum momentum spread. This will correspond to the minimum uncertainty in position. Solving this Fourier transform gives $F(z)$ explicitly as

$$F(z) = \frac{4\pi}{\theta}\exp\left(-\frac{4}{\theta}z\bar{z}\right), \tag{3.17}$$

which is a Gaussian distribution. Despite the maximum spread in momentum, the noncommutativity puts a lower limit, or minimal width, on the uncertainty in position. This motivates choice of matter and charge densities as similar distributions with minimal widths of $\sqrt{\theta}$.

This formulation of noncommutativity solves the violation of unitarity of the $\star$-product [47], and furthermore removes singularities at the origin [4, 33, 37].

The noncommutativity of the manifold encoded in equation 3.2 does not directly imply a natural method for implementing noncommutativity in a model of gravity. While the Moyal product seems to be well motivated by the construction above, there are other mathematically-equivalent, but not necessarily physically-equivalent, products [8]. The choice of a mass distribution in the coherent state formalism as well is not a direct consequence of equation 3.2. However, the argument for its use is well-supported. Firstly, it solves the problem of unitarity, cures UV-divergences, and provides Lorentz invariance [47]. Secondly, the quantum field work above motivates its use. Thirdly, and perhaps the most motivating, is the relationship between a $\star$-product and the gaussian mass distribution: various $\star$-products are mathematically equivalent [8], and can be used to derive the gaussian mass distribution [7, 16].

This derivation is found in [7],[16],[44], and we discuss it briefly here. It relies not on

the Moyal product, but the Voros product

$$f(z,\bar{z}) \star g(z,\bar{z}) = f(z,\bar{z}) \mathrm{e}^{\overleftarrow{\partial_z}\overrightarrow{\partial_z}} g(z,\bar{z}). \tag{3.18}$$

A quantum system is defined as a Hilbert space of (square integrable) wavefunctions $\psi(x)$ over a configuration space R^d, of dimension d.

The aim is to create an equivalent, but noncommutative, quantum system. It is obvious how the above algebra will be modified: the (non-)commutation relation 3.2 will replace the commutative $[\mathbf{X_i}, \mathbf{X_j}] = 0$. The process as follows is taken from [7], which is done in 2-dimensions. The "lifting" to 3-dimensions follows.

This source ([7]), and its reference [44] provide a more detailed derivation of the noncommutative quantum configuration space and noncommutative quantum function space.

States in the noncommutative *configuration* space are denoted $|z\rangle$. When measuring position in a noncommutative space, the best to hope for are states of minimum uncertainty. These are provided by coherent states

$$|z\rangle = \mathrm{e}^{-z\bar{z}/2} \mathrm{e}^{z\mathbf{Z}^\dagger} |0\rangle \tag{3.19}$$

where z is a dimensionless complex number.

The position operators in the noncommutative *function* space are

$$|z,\bar{z}) = \frac{1}{\sqrt{\theta}} |z\rangle\langle z| \tag{3.20}$$

and satisfy the completeness relation

$$\int \frac{\theta \mathrm{d}z\mathrm{d}\bar{z}}{2\pi} = |z,\bar{z}) \star (z,\bar{z}| = \mathbf{1_Q}. \tag{3.21}$$

Here, $\mathbf{1_Q}$ is the identity operator in the quantum space. The star product used here is the Voros product 3.18.

Consider then the overlap of two coherent states, $|\omega,\bar{\omega})$ and $|\zeta,\bar{\zeta})$:

$$(\omega,\bar{\omega}|\zeta,\bar{\zeta}) = \int \frac{\theta \mathrm{d}z\mathrm{d}\bar{z}}{2\pi} (\omega,\bar{\omega}|z,\bar{z}) \star (z,\bar{z}|\zeta,\bar{\zeta}). \tag{3.22}$$

This is satisfied by

$$(\omega,\bar{\omega})|z,\bar{z}) = \frac{1}{\theta}\mathrm{e}^{-r^2/2\theta},\ r = \sqrt{2\theta}\,|w-z|\,. \tag{3.23}$$

The presence of the Voros product replaces the dirac operator with the gaussian distribution above, as

$$\lim_{\theta\to 0} \frac{1}{\theta}\mathrm{e}^{-r^2/2\theta} = 2\pi\delta^{(2)}(r). \tag{3.24}$$

It follows that "lifting" this to 3-dimensions gives the often-used

$$\lim_{\theta\to 0} \frac{1}{(4\pi\theta)^{3/2})}\mathrm{e}^{-r^2/4\theta} = \delta^{(3)}(r). \tag{3.25}$$

We conclude then from these calculations that the Voros product – mathematically equivalent to a Moyal product – implies the replacement of the usual Dirac position-function with the gaussian distribution so often used in current literature.

3.2 Noncommutative spacetimes

As per the previous discussion, we now use a matter distribution of

$$\rho(v,r) = \frac{m(v)}{(4\pi\theta)^{3/2}}\,\mathrm{e}^{-\frac{r^2}{4\theta}}. \tag{3.26}$$

A solution to the Einstein equations is found in the appendix. The process found there is available in many references, which we note there. Solving the Einstein equations with this matter distribution leads us to integrate ρ to give a form of the *lower incomplete gamma function*,

$$\gamma(a,x) = \int_0^a t^{a-1}e^{-t}\,\mathrm{d}t. \tag{3.27}$$

Specifically, the function used is

$$\frac{2}{\sqrt{\pi}}\,\gamma\left(\frac{3}{2},\frac{r^2}{4\theta}\right) = \frac{2}{\sqrt{\pi}}\int_0^{\frac{r^2}{4\theta}} t^{1/2}e^{-t}\,\mathrm{d}t \tag{3.28}$$

The leading coefficient of $2/\sqrt{\pi}$ ensures that for $r\to\infty$, or $r\to 0$, $\frac{2}{\sqrt{\pi}}\gamma\left(\frac{3}{2},\frac{r^2}{4\theta}\right)\to 1$.

3.2.1 Noncommutative Schwarzschild

The noncommutative Schwarzschild metric is [35]

$$ds^2 = -\left(1-\frac{4M\gamma\left(\frac{3}{2},\frac{r^2}{4\theta}\right)}{\sqrt{\pi}\,r}\right)dt^2 + \left(1-\frac{4M\gamma\left(\frac{3}{2},\frac{r^2}{4\theta}\right)}{\sqrt{\pi}\,r}\right)^{-1}dr^2 + r^2d\Omega^2 \tag{3.29}$$

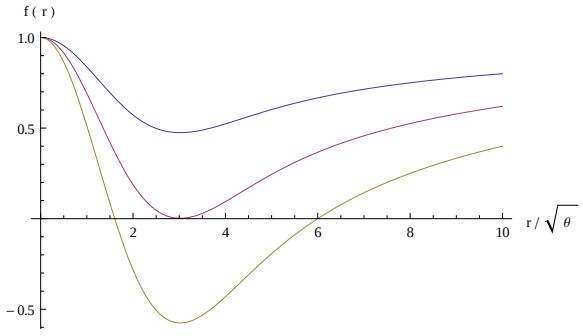

Figure 3.1: The noncommutative Schwarzschild metric function $f(r) = 1 - \frac{4M\gamma\left(\frac{3}{2}, \frac{r^2}{4\theta}\right)}{\sqrt{\pi}\, r}$. Also available in [35].

The addition of the noncommutativity creates changes in the horizon behaviour of the spacetime [35]. For $M \approx 1.9\sqrt{\theta}$, there is one horizon at $r \approx 3\sqrt{\theta}$. For $M < 1.9\sqrt{\theta}$, there is no horizon. For $M > 1.9\sqrt{\theta}$, there are two horizons. For example, when $M = 3\sqrt{\theta}$, there are two horizons at $r_+ \approx 6\sqrt{\theta}$ and $r_- \approx 1.6\sqrt{\theta}$. It is characteristic of noncommutative solutions to have multiple horizons.

In the context of an evaporating (i.e., via Hawking radiation) black hole, the thermodynamic properties are an important consideration. The temperature at the horizon r_H of a noncommutative Schwarzschild black hole was found [37, 32] to be

$$T(r_H) = -\frac{1}{4\pi}\frac{dg_{00}}{dr}\bigg|_{r=r_H} = \frac{1}{4\pi r_H}\left(1 - \frac{r_H^3}{4\theta^{3/2}}\frac{\mathrm{e}^{-\frac{r_H^2}{4\theta}}}{\gamma_H}\right),$$
$$\text{where } \gamma_H = \gamma\left(\frac{3}{2}, \frac{r^2}{4\theta}\right)\bigg|_{r=r_H}. \tag{3.30}$$

More generally, in n-dimensions,

$$T(r_H) = \frac{n+1}{4\pi r_H}\left(1 - \frac{2}{n+1}\left(\frac{r_H}{2\sqrt{\theta}}\right)^{n+3}\frac{\mathrm{e}^{-\frac{r_H^2}{4\theta}}}{\gamma_H^{(n)}}\right) \tag{3.31}$$
$$\text{where } \gamma_H^{(n)} = \gamma\left(\frac{n+3}{2}, \frac{r^2}{4\theta}\right)\bigg|_{r=r_H}. \tag{3.32}$$

Taking the limit $r/\sqrt{\theta} \to \infty$, the classical temperature is recovered, as expected: $T \to \frac{1}{4\pi r_H}$. However, whereas in the classical case the temperature would grow for small r_H, the noncommutative picture is significantly different at small distances. The noncommutative and classical temperatures agree for $r_H > 6\sqrt{\theta}$. As r_H decreases, the noncommutative temperature reaches a maximum of $T \approx 0.015 \times 1\sqrt{\theta}$ at approximately $M \approx 2.4\sqrt{\theta}$; thereafter, the temperature decreases to zero at $M \approx 3\sqrt{\theta}$ which corresponds to the extremal (single-horizon) black hole [37]. At higher dimensions, the result is similar: there is a maximum temperature that increases with the dimension; the minimal mass with zero-temperature decreases at higher dimensions [36].

As r decreases, the curvature is non-vanishing and positive [37],

$$R(0) = \frac{4M}{\sqrt{\pi}\theta^{3/2}} \tag{3.33}$$

which is equivalent to a deSitter geometry. The singularity is *removed* at the origin, and replaced by a deSitter core.

3.2.1.1 Noncommutative Schwarzschild-deSitter

The analysis of this black hole solution can be found in Mann and Nicolini [27], and we mention their results briefly.

The noncommutativity creates two black hole horizons as in the non-cosmological Schwarzschild solution, and the presence of a cosmological constant Λ adds a cosmological horizon. The horizon behaviour is dependant on M and Λ, and there are four cases. There is a minimal mass M_0 such that $M < M_0$ shows only a cosmological horizon. When $M = M_0$, the two black hole horizons combine, and there is

still a cosmological horizon. For $M > M_0$, there is a critical value M_N such that when $M = M_N$, the outer black hole horizon and the cosmological horizon combine into a Nariai-like solution. Otherwise, for all $M > M_0$, there are three horizons: a cosmological horizon, and two black hole horizons.

The Nariai solution has a line-element

$$ds^2 = \frac{1}{A}\left(d\chi^2 + \sin^2\chi d\psi^2\right) + \frac{1}{B}\left(d\vartheta^2 + \sin^2\vartheta d\phi^2\right) \tag{3.34}$$

where A and B are constants, $\chi, \vartheta \in [0, \pi]$, and ψ and ϕ are periodic coordinates with period 2π. This topology is clearly $S^2 \times S^2$.

3.2.2 Noncommutative Reissner-Nordström

A noncommutative Reissner-Nordström [4] is similar to the Schwarzschild construction in that the matter, and now electric, fields are diffused over a Gaussian distribution,

$$\begin{aligned} \rho_{\text{matt}}(r) &= \frac{M}{(4\pi\theta)^{3/2}} \mathrm{e}^{-\frac{r^2}{4\theta}} \\ \rho_{\text{el}}(r) &= \frac{Q}{(4\pi\theta)^{3/2}} \mathrm{e}^{-\frac{r^2}{4\theta}} \end{aligned} \tag{3.35}$$

Using a 4-current of

$$J^\alpha = \rho_{\text{el}} \delta^\alpha{}_0 \tag{3.36}$$

and Maxwell's equations

$$\begin{aligned} F^{\alpha\beta} &= \delta^{0[\alpha|}\delta^{r|\beta]} E(r) \\ J^\alpha &= \frac{1}{\sqrt{-g}} \partial_\beta \left(\sqrt{-g} F^{\alpha\beta}\right) \end{aligned} \tag{3.37}$$

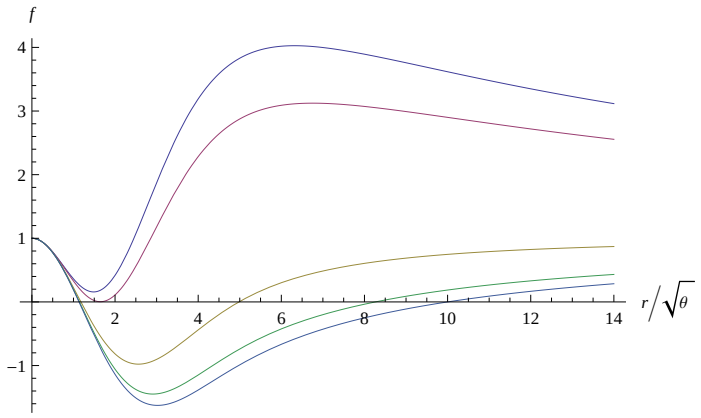

Figure 3.2: The noncommutative Reissner-Nordström metric function with $Q = kM$, $M = 5\sqrt{\theta}$, with $k \in \{0, 0.5, 1, 1.97, 2.2\}$ increasing from bottom to top.

More explicitly, $F^{0r} = E(v, r) = -F^{r0}$, and $F^{\alpha\beta} = 0$ otherwise. Solving Maxwell's equations gives

$$E(r) = \frac{Q}{8\pi\theta^{3/2}r^2}\gamma\left(\frac{3}{2}, \frac{r^2}{4\theta}\right) \tag{3.38}$$

Solving Einstein's equations with $E(r)$ as above gives a metric function

$$f(r) = 1 - \frac{4M\gamma\left(\frac{3}{2}, \frac{r^2}{4\theta}\right)}{\sqrt{\pi}r} + \frac{Q^2}{\pi r^2}\left(\gamma\left(\frac{1}{2}, \frac{r^2}{4\theta}\right)^2 - \frac{r}{\sqrt{2\theta}}\gamma\left(\frac{1}{2}, \frac{r^2}{2\theta}\right)\right). \tag{3.39}$$

The appendix to this work demonstrates in more detail the solution process.

Horizons are presented in Figure 3.2 with Q ranging from zero, up to the classically-extremal $Q = M$, and beyond: $Q > M$. Note that for $Q < M/2$ there is little effect on the outer horizon as compared to the $Q = 0$ case. For $Q = M$, the horizon is indeed at M. For $Q > M$, there is a critical value of about $Q \approx 1.97M$, at which point the black hole is "extremal": there is a single horizon at about $r = 1.64\sqrt{\theta}$. For still larger Q, there is no horizon.

Chapter 4

Noncommutative modifications to the Vaidya spacetime

We now consider a generalized Vaidya spacetime, that also includes noncommutative effects. By generalized, we mean that the solution allows for both mass and charge. In null coordinates, the generalized form is

$$ds^2 = -f(v,r)dv^2 + 2dvdr + r^2(d\vartheta^2 + \sin^2\vartheta d\phi^2) \tag{4.1}$$

$$f(v,r) = 1 - \frac{2M(v,r)}{r} + \frac{Q(v,r)^2}{r^2} \tag{4.2}$$

where v is an ingoing null coordinate. The functions $M(v,r)$ and $Q(v,r)$ are both dependent on v (so that the mass and charge either increase or decrease), and r (knowing that noncommutativity will diffuse both mass and charge over a width of $\sqrt{\theta}$).

We will be adding noncommutativity in terms of a mass and charge distribution of

$$\rho_M(v,r) = \frac{m(v)}{4\pi\theta^{3/2}}\mathrm{e}^{-r^2/4\theta} \tag{4.3}$$

$$\rho_Q(v,r) = \frac{q(v)}{4\pi\theta^{3/2}}\mathrm{e}^{-r^2/4\theta} \tag{4.4}$$

The charge density is only along the v-direction, and is given by

$$J^\alpha = \rho_Q(v,r)\delta^{\alpha 0} \tag{4.5}$$

Solving the Einstein equations with the above choices (details in the appendix) gives the expected metric function

$$f(v,r) = 1 - \frac{4m(v)}{\sqrt{\pi}r}\gamma\left(\frac{3}{2},\frac{r^2}{4\theta}\right) + \frac{q(v)^2}{\pi r^2}\left(\gamma\left(\frac{1}{2},\frac{r^2}{4\theta}\right)^2 - \frac{r}{\sqrt{2\theta}}\gamma\left(\frac{1}{2},\frac{r^2}{2\theta}\right)\right) \tag{4.6}$$

The metric function above is equivalent to the noncommutative Reissner-Nordström solution [4] in null coordinates, but with time-dependent mass and charge.

Given that we are using a generalized solution, we aim to describe its behaviour as fully as possible. While current literature has investigated the case of black hole evaporation in a static solution and as well in a limited Vaidya context, and the associated thermodynamics, we will be describing the other side of the coin, namely, black hole formation. We shall examine the characteristic horizon behaviour, restrictions on energy conditions, and extremal behaviour. We finish with a new solution that satisfies otherwise-violated energy conditions.

Noncommutative Vaidya solutions have already been considered [29, 28, 32], though in explicit (t,r) coordinates for black-hole evaporation. The metric has a similar

form, though the mass function is prescribed by the solution. The mass function in the explicit $(t-r)$ case reads

$$M_\theta = M_I \left[\mathcal{E}\left(\frac{r-t}{2\sqrt{\theta}}\right)\left(1+\frac{t^2}{2\theta}\right) - \frac{r}{\sqrt{\pi\theta}} \mathrm{e}^{-\frac{(r-t)^2}{4\theta}} \left(1+\frac{t}{r}\right)\right], \tag{4.7}$$

where M_I is the initial mass, and $\mathcal{E}$ is the Gauss error function,

$$\mathcal{E}(n) = \frac{2}{\sqrt{\pi}} \int_0^n \mathrm{e}^{-p^2} dp. \tag{4.8}$$

In the limit of $r/\sqrt{\theta} \to \infty$, the mass function becomes

$$M_\theta = M_I \left(1+\frac{t^2}{2\theta}\right). \tag{4.9}$$

The stationary case is recovered for $t=0$, and M_θ is the noncommutative mass,

$$M_\theta = M_I \left(\frac{2}{\sqrt{\theta}} \gamma\left(\frac{3}{2}, \frac{r^2}{4\theta}\right)\right). \tag{4.10}$$

We choose however to work in the usual Eddington-Finkelstein-type coordinates. As such, we are free to choose a mass function $M_I(v)$. As well, we wish to model mass accretion ($\dot{m}(v) > 0$), rather than black hole evaporation ($\dot{m}(v) < 0$).

We choose an appropriate mass function, based on the error function such as

$$m(v) = \frac{m_f - m_0}{2} \left(1 + \mathcal{E}\left(v\right)\right) + m_0 \tag{4.11}$$

for an initial mass m_0 and a final mass m_f.

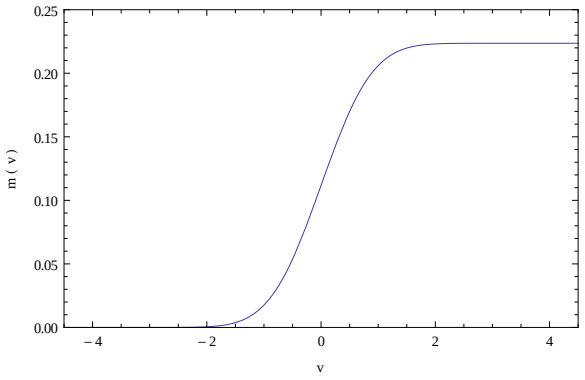

Figure 4.1: The chosen mass function $m(v) = \frac{m_f}{2}\left(1 + \mathcal{E}\left(v\right)\right)$ for $m_f = 1\sqrt{\theta}$.

This could easily model an existing object accreting further mass; however, to represent the formation of a black hole we will be assuming $m_0 = 0$. This gives

$$m(v) = \frac{m_f}{2}\left(1 + \mathcal{E}\left(v\right)\right) \tag{4.12}$$

For $v \to -\infty$, $m(v) \to 0$; for $v \to \infty$, $m(v) \to m_f$. The transition from 0 to m_f occurs over the approximate interval $v \in (-4, 4)$.

Before beginning detailed analysis, a discussion of appropriate numerical values is needed. Mass, charge, and radial distance are equivalent units, so then m/r, q/r are dimensionless. They are also scaled in multiples of $\sqrt{\theta}$. Since everything is scaled to multiples of $\sqrt{\theta}$, the actual value of $\sqrt{\theta}$ is relatively unimportant, and we can consider it to be simply ℓ_P. We will be working with $\sqrt{\theta} = \sqrt{0.05}$. It should be noted that while choosing smaller $\sqrt{\theta}$ will still illustrate the same characteristic behaviour presented below, choosing *larger* values ($\sqrt{\theta} \approx 1$) does in fact change the overall behaviour.

4.1 Horizons

One characteristic of a noncommutative modification to a spacetime is that extra horizons are created. In a generalized case, we are dealing with multiple variables (i.e. time, mass, charge, cosmological constant) that can interact and affect the formation of horizons. The situation is not as complicated as may seem, as the dependence of one quantity on another is predictable.

4.1.1 Uncharged Vaidya

We begin with the uncharged Vaidya solution. While this has been considered within the context of Hawking evaporation, we are considering black hole formation with a different mass function. Note that many of the properties discussed below are in line with the noncommutative Schwarzschild black hole discussed in [35].

Recall our mass function,

$$m(v) = \frac{m_f}{2}(1 + \mathcal{E}(v)) \tag{4.13}$$

For $v \leq -4$, $m(v) \approx 0$; for $v \geq 4$, $m(v) \approx m_f$. This dictates our choice of interval $v \in (-4, 4)$. Note as well that for $r/\sqrt{\theta} \gtrapprox 8$, $\frac{2}{\sqrt{\pi}}\gamma\left(\frac{3}{2}, \frac{r^2}{4\theta}\right) \approx 1$. Depending on the solution being considered, any horizon at $r/\sqrt{\theta} > 8.02$ may indeed coincide with the classical horizon.

The noncommutative Schwarzschild-Vaidya solution has metric function

$$f(v, r) = 1 - \frac{2m(v)(1 + \mathcal{E}(v))}{\sqrt{\pi} r}\,\gamma\left(\frac{3}{2}, \frac{r^2}{4\theta}\right) \tag{4.14}$$

Apparent horizons, and event horizons, are plotted below in Figure 4.2. Note that for $r \approx 2.7 \approx 12.3\sqrt{\theta}$, the classical (i.e. commutative) horizon coincides with the

noncommutative horizon at that same location. Recall that for $r > 8.02\sqrt{\theta}$, the noncommutative effects disappear. Accordingly, the event horizons of both the classical and noncommutative solutions also coincide. A secondary interior horizon is found at $r = \sqrt{\theta}$. Our selective choice of mass has made this determination explicit: $m_f = \frac{\sqrt{\pi}}{4}\gamma\left(\frac{3}{2}, \frac{1}{4}\right)^{-1}\sqrt{\theta}$.

For $v > 4$, the spacetime is essentially static. The metric function is then

$$\begin{aligned} f &= 1 - \frac{4m_f}{\sqrt{\pi}}\frac{\gamma\left(\frac{3}{2}, \frac{r^2}{4\theta}\right)}{r} \\ &= 1 - \frac{\gamma\left(\frac{3}{2}, \frac{r^2}{4\theta}\right)}{\gamma\left(\frac{3}{2}, \frac{1}{4}\right)}\frac{\sqrt{\theta}}{r} \end{aligned} \tag{4.15}$$

which is zero at $r = \sqrt{\theta}$. Certainly for other masses, this determination is not explicit. The horizon location is found from the more general statement [35]

$$\left(\frac{2}{\sqrt{\pi}}\gamma\left(\frac{3}{2}, \frac{r^2}{4\theta}\right)\right)^{-1} r = 2m_f \tag{4.16}$$

For large r (i.e. $r > 8.02\sqrt{\theta}$), this reduces to the usual $r = 2m_f$. Unfortunately, for smaller r, the nature of the gamma function makes explicit analytic solutions difficult.

It has been shown recently that these interior horizons are Cauchy horizons, and unstable [10].

As previously noted, for $m_f > 1.9\sqrt{\theta}$, there are two horizons. When m_f is chosen to be progressively larger, the interior horizon decreases in r, while $r = 2m_f$ is, of course, still the exterior horizon. This is evident from Figure 3.1, and is discussed in [35].

This begs the question at what value of m_f would the noncommutative effects not be discernible? Assuming that $\sqrt{\theta} = \ell_P$, any horizon $r < \ell_P$ is met with skepticism,

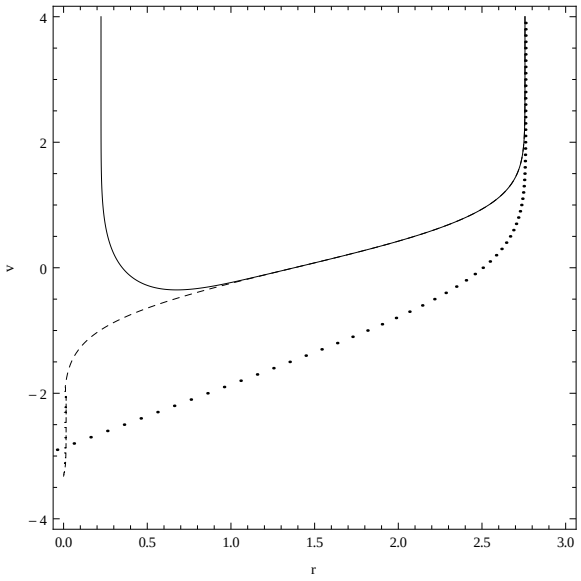

Figure 4.2: Horizons of a Schwarzschild-Vaidya solution, for $m_f = \frac{\sqrt{\pi}}{4}\left(\gamma\left(\frac{3}{2},\frac{1}{4}\right)\right)^{-1}$. (Solid - Noncommutative; Dashed - Classical; Dotted - Event horizon

simply due to the quantization of space, where the minimum length is ℓ_P. There is no meaning in a horizon at $r < \ell_P$. What is the maximum mass that would allow an inner horizon to be "observable"? Of course, in posing that question, we are ignoring that we are in the interior of a black hole! In the Schwarzschild case, $m_f = \frac{\sqrt{\pi}}{4}\gamma\left(\frac{3}{2},\frac{r^2}{4\theta}\right)^{-1}\sqrt{\theta}$ ensures this requirement; we have also presented the more general requirement in Equation 4.16.

4.1.2 Charged Vaidya

The addition of electric charge significantly complicates the metric function, where the line element has the function

$$f(v,r) = 1 - \frac{4m(v)}{\sqrt{\pi}r}\gamma\left(\frac{3}{2},\frac{r^2}{4\theta}\right) + \frac{q(v)^2}{\pi r^2}\left(\gamma\left(\frac{1}{2},\frac{r^2}{4\theta}\right)^2 - \frac{r}{\sqrt{2\theta}}\gamma\left(\frac{1}{2},\frac{r^2}{2\theta}\right)\right) \qquad (4.17)$$

Again, this solution shares characteristic behaviour with the static noncommutative Reissner-Nordström discussed in [4].

Considering first the classical static solution, there are at most two solutions, or one in the extremal case. The metric function

$$f(r) = 1 - \frac{2M}{r} + \frac{Q^2}{r^2} \tag{4.18}$$

has solutions at

$$r_H = \left(M \pm \sqrt{M^2 - Q^2} \right) \tag{4.19}$$

which mandates that for a given charge Q, the smallest mass possible is $M = Q$. This is the extremal case; we shall see later that no similar restriction is as easily found for the noncommutative case. To avoid possible issues in this way, we shall choose an appropriate mass-to-charge ratio.

Assuming that charge will grow at an equal rate to mass, we use a similar charge function, $q(v) = \frac{q_f}{2}(1+\mathcal{E}(v))$. Considering Figure 4.3, we see that as mass and charge accumulate, the classical solution begins as a single horizon at $r = 0$, bifurcating to the two expected horizons. The noncommutative solution, while having a similar event horizon, has an apparent horizon appearing later in v and shifted in r, at $r \approx 2.1M$.

The maximum mass that ensures $(v, r) = (\infty, \sqrt{\theta})$ is a horizon is the solution to

$$1 - \frac{4m_f}{\pi\sqrt{\theta}}\gamma\left(\frac{3}{2}, \frac{1}{4}\right) + \frac{q_f^2}{\pi\theta}\left(\gamma\left(\frac{1}{2}, \frac{1}{4}\right) - \frac{1}{\sqrt{2}}\gamma\left(\frac{1}{2}, \frac{1}{2}\right)\right) = 0 \tag{4.20}$$

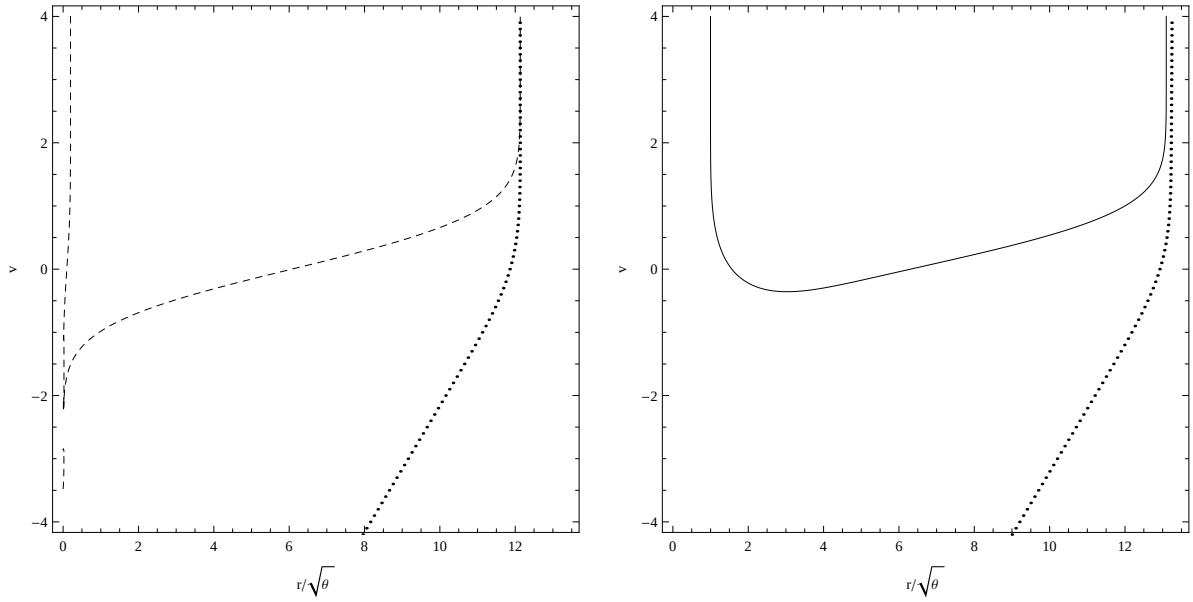

Figure 4.3: Horizons of a charged Vaidya solution, for $m_f = \frac{\sqrt{\pi}}{4}\left(\gamma\left(\frac{3}{2},\frac{1}{4}\right)\right)^{-1}$ and $q_f = m_f/4$. Classical at left, noncommutative at right.

which is

$$\begin{aligned}\frac{m_f}{\sqrt{\theta}} &= \frac{q_f^2}{4\theta}\gamma\left(\frac{3}{2},\frac{1}{4}\right)^{-1}\left(\gamma\left(\frac{1}{2},\frac{1}{4}\right)^2 - \frac{1}{\sqrt{2}}\gamma\left(\frac{1}{2},\frac{1}{2}\right)\right) + \frac{\pi}{4} \\ &\approx 0.785 - 0.063\left(\frac{q_f}{\sqrt{\theta}}\right)^2 \end{aligned} \tag{4.21}$$

To ensure $m_f \geq 0$, $q \leq 7.08\sqrt{\theta}$. There is no clear requirement that $m > q$, as in the classical case. Shown in 4.4 is the case where $m = q/2$.

What will determine whether this is an acceptable choice of values for m_f and q_f is the energy conditions, which will be examined later. This will not be a clear-cut conclusion, however, as the nature of the noncommutativity will often break the energy conditions. As well, extremality will need a better definition than the classical, and utilitarian, "$m = q$" that is often used.

Another aspect to consider carefully is the effect of the noncommutativity on the

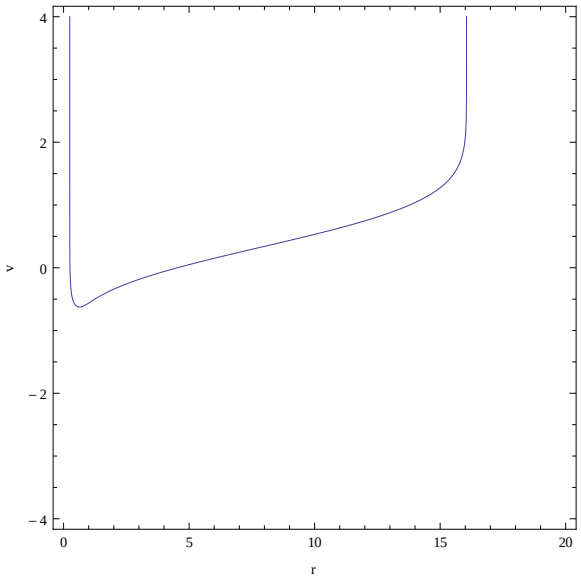

Figure 4.4: Horizons of charged Vaidya solution, for $m_f = q_f/2$

nature of the matter and electric fields. As chosen, the matter field is distributed across a region of width $\sqrt{\theta}$:

$$f(v,r) = \ldots - \frac{4m(v)\gamma\left(\frac{3}{2}, \frac{r^2}{4\theta}\right)}{\sqrt{\pi}r} \ldots \tag{4.22}$$

In the limit $r/\sqrt{\theta} \to \infty$, this term becomes the classical mass term, $-2m/r$.

Consider next the noncommutativity factor of the charged term of the metric function:

$$\begin{aligned} f(v,r) &= \ldots \frac{Q(v,r)^2}{\pi r^2}\left(\gamma\left(\frac{1}{2}, \frac{r^2}{4\theta}\right)^2 - \frac{r}{\sqrt{2\theta}}\gamma\left(\frac{1}{2}, \frac{r^2}{2\theta}\right)\right) \\ &= \ldots \frac{Q(v,r)^2}{\pi r^2}\gamma\left(\frac{1}{2}, \frac{1}{4}\left(\frac{r}{\sqrt{\theta}}\right)^2\right) - \frac{Q(v,r)^2}{\pi(r/\sqrt{\theta})}\frac{1}{\sqrt{2\theta}}\gamma\left(\frac{1}{2}, \frac{1}{2}\left(\frac{r}{\sqrt{\theta}}\right)^2\right) \end{aligned} \tag{4.23}$$

In the limit $r/\sqrt{\theta} \to \infty$, the second term above goes to zero, while the first becomes the expected Q/r^2. That being said, however, the small-scale behaviour of this term is worth investigating.

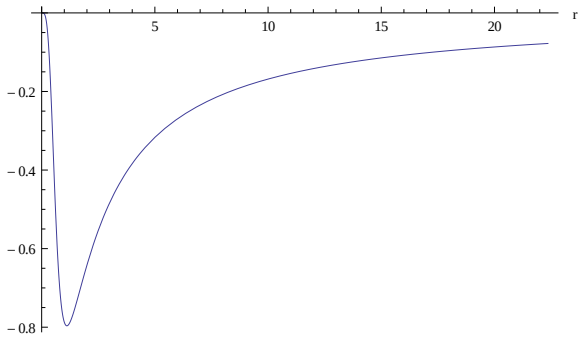

Figure 4.5: Detail of charge term in noncommutative Reissner-Nordström

Factoring $q(v)$ out of the expression, we see that the term is always negative; see Figure 4.5. For large r, the expression tends to zero, which is to be expected: $Q/r^2 \to 0$ as well for large r. At issue here, however, is that the sign of the expression adjusts the location of the apparent horizon. In the classical, commutative, sub-extremal Reissner-Nordström solution, there are two horizons, given by

$$r_H = M \pm \sqrt{M^2 - Q^2}. \tag{4.24}$$

In the noncommutative case, an analogous pair of horizons does not exist. Indeed, there is an interior horizon, but we identify this as the noncommutative horizon that appears in even the non-charged Schwarzschild case.

The presence of the noncommutative charged term extends the horizon outward, as seen in the comparative Figure 4.6. The outer horizon presented in this Figure is the apparent horizon for the noncommutative charged Vaidya, while the horizon at a slightly smaller value of r is the apparent horizon for the noncommutative (uncharged) Vaidya solution. Both solutions have an identical inner horizon, formed by the noncommutativity.

The fact that there is only a single "outer" horizon for the charged Vaidya solution

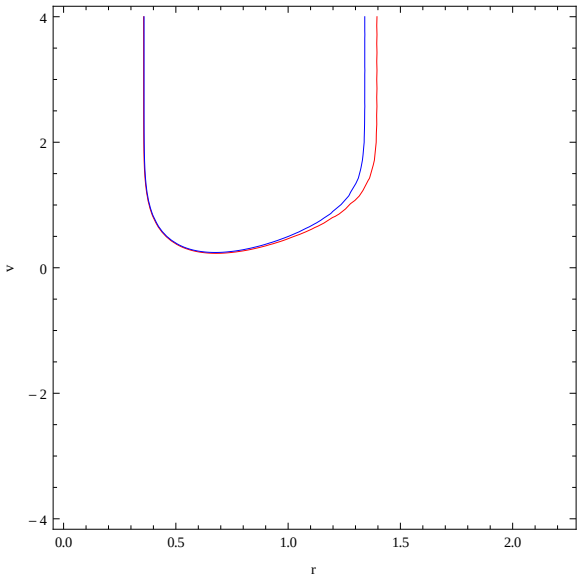

Figure 4.6: Detail of the apparent horizons for noncommutative Vaidya (inner) and noncommutative charged Vaidya (outer). ($m = 3\sqrt{\theta}$, $q = m/3$)

begs the question: In what scenario will the second outer (classical) horizon form? Let us begin with a comparison for small mass, $m = 3\sqrt{\theta}$. As shown in Figure 4.7, we see the characteristic U-shape of the noncommutative horizons. The outer horizon is at a slightly larger radius than $r = 2m$; this is a noncommutative effect.

The noncommutative model begins to fail for very large values of M, regardless of the choice of Q. It would be expected that for large values of M and Q, the model should smoothly transition to the classical, commutative, model. This is not the case. Even more problematic is the lack of agreement in apparent horizon. If mass and charge are both very large, say $M = 3000\sqrt{\theta}$, with $Q = M/3$, then $r_H = M + \sqrt{M^2 - Q^2} \approx 5828\sqrt{\theta}$ is a poor approximation to the outer horizon. The "fuzziness" created by the noncommutativity shifts the horizon location to such a great extent that the outer horizon cannot be trusted as accurate. Consider the Figure 4.8. We would expect the outer horizon to be at $r_H \approx 5828\sqrt{\theta}$, but instead, the horizon is found at approximately $r_H \approx 90000 \approx 402492\sqrt{\theta}$!

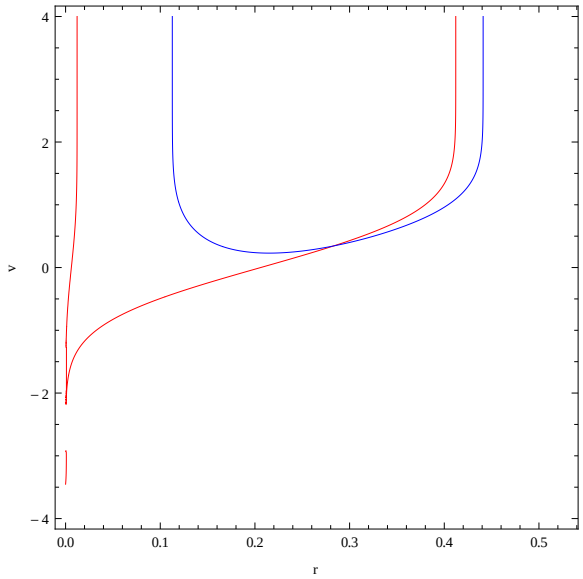

Figure 4.7: Comparison of apparent horizons for the classical and noncommutative (U-shaped) charged Vaidya solutions.

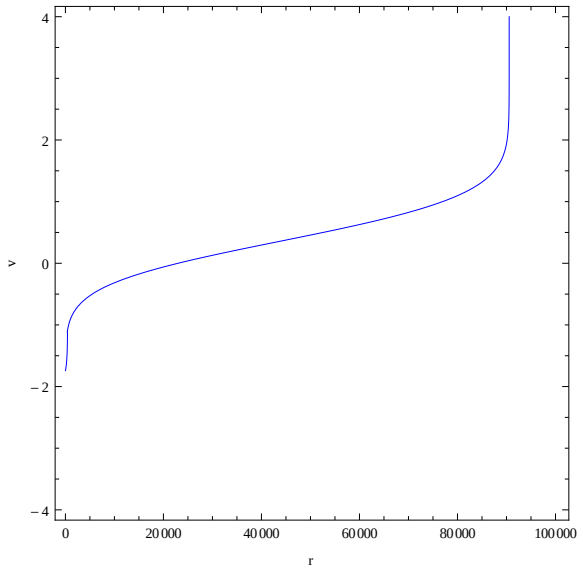

Figure 4.8: Noncommutative charged Vaidya for large mass, $M = 3000\sqrt{\theta}$. The charge is $Q = M/3$.

There is evidently an issue of scale in the applicability of the noncommutative model. One would expect that the model should smooth transition to the large-scale commutative model in the appropriate limit. Certainly, for $r/\sqrt{\theta} \to \infty$, the model does indeed transition correctly. However, simply choosing M (and Q) large does not have the same effect. Since we are considering a dynamic model, it would be reasonable to assume that as M (and Q) grow sufficiently large, then the noncommutative effect would decrease at a proportional rate, so that the model would describe both the small-scale and large-scale scenarios correctly. As seen, the apparent horizon location is incorrect for large M (and Q).

There is a second issue to consider as well, apart from the horizon at $r \gg 2M$. In the classical Reissner-Nordström, there is a second interior Cauchy horizon, evidenced from the solution $r = M \pm \sqrt{M^2 - Q^2}$. There is no such horizon for small or large M and Q. There is certainly an interior horizon, at $r \approx 1\sqrt{\theta}$, but as this horizon is found in the Schwarzschild solution as well, we can safely assume it to be the noncommutative horizon. So where is the second outer horizon? It simply does not exist, for any values of M and Q, large or small.

Finally, the electric field Q is also partially acting as a mass term. Consider the electric term in the metric function,

$$f(v,r) = \ldots \frac{q(v)^2}{\pi r^2}\left(\gamma\left(\frac{1}{2}, \frac{r^2}{4\theta}\right)^2 - \frac{r}{\sqrt{2\theta}}\gamma\left(\frac{1}{2}, \frac{r^2}{2\theta}\right)\right) \tag{4.25}$$

Expand this, and see that the second term behaves as an effective mass of $q(v)^2/\pi\sqrt{2\theta}$.

$$f(v,r) = \ldots \frac{q(v)^2}{\pi r^2}\gamma\left(\frac{1}{2}, \frac{r^2}{4\theta}\right)^2 - \frac{q(v)^2}{\pi r\sqrt{2\theta}}\gamma\left(\frac{1}{2}, \frac{r^2}{2\theta}\right) \tag{4.26}$$

Thus, the metric can be interpreted as

$$f(v,r) = 1 - \left(\frac{4m(v)}{\sqrt{\pi} r} \gamma\left(\frac{3}{2}, \frac{r^2}{4\theta} \right) + \frac{q(v)^2}{\pi r \sqrt{2\theta}} \gamma\left(\frac{1}{2}, \frac{r^2}{2\theta} \right) \right) + \frac{q(v)^2}{\pi r^2} \gamma\left(\frac{1}{2}, \frac{r^2}{4\theta} \right)^2 \quad (4.27)$$

Over the r-axis, what dominates: mass, or charge? For large r, the gamma function has limits

$$\lim_{x \to \infty} \gamma\left(\frac{1}{2}, x \right) = \sqrt{\pi} \quad (4.28)$$

$$\lim_{x \to \infty} \gamma\left(\frac{3}{2}, x \right) = \frac{\sqrt{\pi}}{2} \quad (4.29)$$

We then solve the following inequality to find an upper limit on Q. We assume that $M \geq 1\sqrt{\theta}$.

$$\frac{4M}{\sqrt{\pi} r} \gamma\left(\frac{3}{2}, \frac{r^2}{4\theta} \right) \geq \frac{Q^2}{\pi r \sqrt{2\theta}} \gamma\left(\frac{1}{2}, \frac{r^2}{2\theta} \right) \quad (4.30)$$

For large r, the mass parameter will dominate when

$$Q^2 \leq \sqrt{8\pi\theta} M \approx 5\sqrt{\theta} M. \quad (4.31)$$

As of yet, there is no noncommutative-based restriction on Q such as is found in the classical case ($Q \leq M$). As well, at small r, the charge term will dominate. Refer to Figure 4.9. For increasing r, the mass term will "eventually" overtake the charge term, but there is still a region of small r where the charge contributes most to what we may consider the "mass" of the black hole. Without a good definition of local mass, it is difficult to say what mass is measured for small or large r. Generally, mass is defined as what is measured at infinity, though this is not always well defined in a dynamic spacetime.

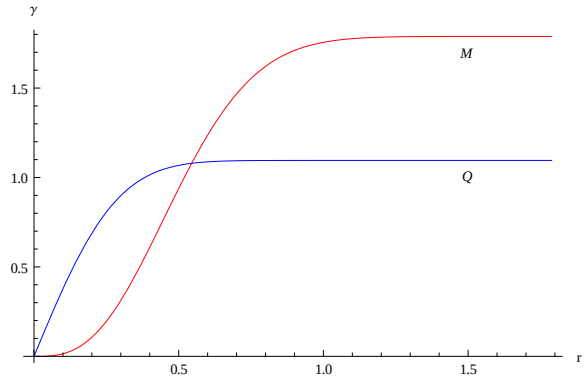

Figure 4.9: Comparison of mass and charge as effective-mass terms in a noncommutative Reissner-Nordström black hole. Here $Q^2 = \sqrt{3\pi\theta}M$.

When a black hole and the spacetime are time-dependent, the determination of mass is not as clear. If the mass of the black hole stabilizes at late times, then there is the usual global definition of mass for the entire spacetime. If the mass of the black hole is changing, then it is difficult to determine a local mass for the black hole, and its relation to the mass of the spacetime measured at infinity. Nevertheless, we still call the mass parameter of a black hole its "mass" out of convenience, due to a lack of a universally-applicable and precise definition of mass.

4.2 Extremality

We now return to a *static* form of a noncommutative metric. As was already noted for both noncommutative Schwarzschild and Reissner-Nordström metrics, two horizons exist for any mass above a critical value. At that critical/minimal value, the black hole has a single horizon. Our aim is to determine the location of this point, and then show its correspondence to a dynamic black hole. We shall call the black hole "extremal" when the mass is at this critical value. While this black hole state may not correspond to the strictest use of the term "extremal", we are using it in its more

general sense: it represents a minimal mass at which a single horizon exists, rather than two. This is analogous to the classical Reissner-Nordström solution, where a single horizon exists when the charge-to-mass ratio is one, and two horizons exist for any ratio less than one. One could characterize an extremal Reissner-Nordström black hole as one where the mass reaches a minimum relative to the charge.

4.2.1 Static noncommutative Reissner-Nordström

Assuming a static Reissner-Nordström metric, there exists a minimal mass at which a single horizon forms, for some choice of M and Q. While it is not possible to analytically determine horizon locations in a noncommutative solution, are we able to determine some form of relation between M, Q, and horizon radius r_H at this point of extremality?

In the classical case, we can easily turn to the horizon location,

$$r_H = M \pm \sqrt{M^2 - Q^2} \tag{4.32}$$

which gives two horizons, except when $M = Q$, and there is a single horizon. In a noncommutative case there is no easy explicit statement for the horizons. Moreover, the square-root in the above equation limits the relative sizes of M and Q so that $M = Q$ is the smallest mass (largest charge) possible. There is no such limitation on the noncommutative Reissner-Nordström case.

Recall first the metric function,

$$f(r) = 1 - \frac{4M}{\sqrt{\pi} r}\gamma\left(\frac{3}{2}, \frac{r^2}{4\theta}\right) + \frac{Q^2}{\pi r^2}\left(\gamma\left(\frac{1}{2}, \frac{r^2}{4\theta}\right)^2 - \frac{r}{\sqrt{2\theta}}\gamma\left(\frac{1}{2}, \frac{r^2}{2\theta}\right)\right). \tag{4.33}$$

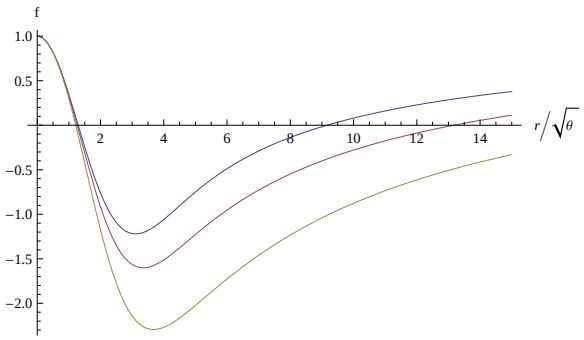

Figure 4.10: The noncommutative Reissner-Nordström metric function for $Q = 0.5M$; $Q = M$; $Q = 1.5M$.

Presented in Figure 4.10 are three graphs of the metric function f for the choice of parameters, $M < Q$, $M = Q$ and $M > Q$, in order from top to bottom.

This is certainly not the picture we would expect in a classical case, considering that there are consistently roots, indicating horizons, for all Q/M ratios necessarily less than one. While finding the location of a horizon, albeit numerically, is indeed possible, we aim to find some kind of relation between the three parameters of the extremal case: (M, Q, r_H).

Let ξ^α be a Killing vector scaled so that $\xi^2 \to -1$ at spatial infinity. The geodesic acceleration, or inaffinity (measure of "affine-ness"), is then defined as the solution to the equation [50]

$$\xi^\beta \nabla_\beta \xi^\alpha = \kappa \xi^\alpha. \tag{4.34}$$

This vector is tangent to the geodesics generating the horizon. We call κ the surface gravity. The surface gravity may be non-zero; if the black hole is *extremal*, then $\kappa = 0$.

Since we are considering a static case, we can choose $\xi^\alpha = (1, 0, 0, 0)$ as an acceptable Killing vector. Assuming this vector, the spacetime in null coordinates, and a metric

function $f(r)$, the equation 4.34 has solution

$$\kappa = \frac{1}{2}\partial_r f(r) \tag{4.35}$$

The surface gravity of a black hole is always positive, but equal to zero in the extremal case. For example, the Schwarzschild spacetime has surface gravity

$$\kappa = \frac{1}{2}\partial_r \left(1 - \frac{2M}{r}\right)_{r=2M} = \frac{1}{4M}, \tag{4.36}$$

which is evidently positive. There is no "extremal Schwarzschild" possible. On the other hand, a Reissner-Nordström black hole has surface gravity

$$\begin{aligned} \kappa &= \frac{1}{2}\partial_r \left(1 - \frac{2M}{r} + \frac{Q^2}{r^2}\right) \\ &= \frac{M}{r^2} - \frac{Q^2}{r^3} \\ &= \frac{1}{r^3}\left(Mr - Q^2\right) \end{aligned} \tag{4.37}$$

When $r = M = Q$, $\kappa = 0$. Recall that $r = M$ is the event horizon of the extremal Reissner-Nordström black hole, when $Q/M = 1$.

Considering the noncommutative Schwarzschild case, the surface gravity is

$$\kappa = m\left(\frac{2\gamma\left(\frac{3}{2}, \frac{r^2}{4\theta}\right)}{\sqrt{\pi}r^2} - \frac{\mathrm{e}^{\left(-\frac{r^2}{4\theta}\right)}r}{2\sqrt{\pi}\theta^{3/2}}\right) \tag{4.38}$$

We now see in Figure 4.11 that the addition of noncommutativity renders $\kappa < 0$ for the approximate region $(0, 3\sqrt{\theta})$, and positive there-after. Of interest is that the areal radius where $\kappa = 0$ is independent of the final mass, as can be seen in equation

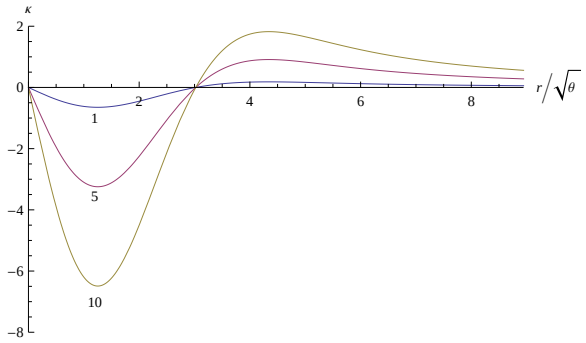

Figure 4.11: Plot of κ for the Schwarzschild black hole, for mass parameter $m/\sqrt{\theta} \in \{1, 5, 10\}$. The ratio $m/\sqrt{\theta}$ is indicated on the graph.

4.38. Solving Equation 4.38 for $\kappa = 0$, we find $r \approx 3\sqrt{\theta}$. In contrast to the classical Schwarzschild and Reissner-Nordström solutions, we see that κ vanishes, not for a fixed mass, but instead is independent of that mass parameter. We will return to this result again in the context of a dynamic solution.

Next, the Reissner-Nordström solution has acceleration

$$\begin{aligned}\kappa = M &\left(\frac{\gamma\left(\frac{1}{2}, \frac{r^2}{r\theta}\right)}{\sqrt{\pi}r^2} - \frac{\mathrm{e}^{\frac{-r^2}{4\theta}}\left(r^2 + 2\theta\right)}{2\sqrt{\pi}\theta^{3/2}r}\right) \\ + Q^2 &\left(-\frac{\mathrm{e}^{-\frac{r^2}{2\theta}}}{2\pi\theta r} - \frac{\left(\gamma\left(\frac{1}{2}, \frac{r^2}{4\theta}\right)\right)^2}{\sqrt{\pi}r^3} + \frac{4\mathrm{e}^{-\frac{r^2}{4\theta}}\gamma\left(\frac{1}{2}, \frac{r^2}{4\theta}\right) + \sqrt{2}\gamma\left(\frac{1}{2}, \frac{r^2}{2\theta}\right)}{4\pi\sqrt{\theta}r^2}\right).\end{aligned} \tag{4.39}$$

We expect from Equation 4.39 that there will be multiple solutions of (M, Q, r_H) that satisfy $\kappa = 0$. Furthermore, we want the metric function to be satisfied as well, ensuring that r labels the horizon: $f(M, Q, r_H) = 0$. The requirement on an extremal horizon is then that

$$\begin{aligned} f(r_H) &= 0 \\ \kappa(r_H) &= 0 \end{aligned} \tag{4.40}$$

for some r_H, the horizon. In a classical Reissner-Nordström black hole, there is a

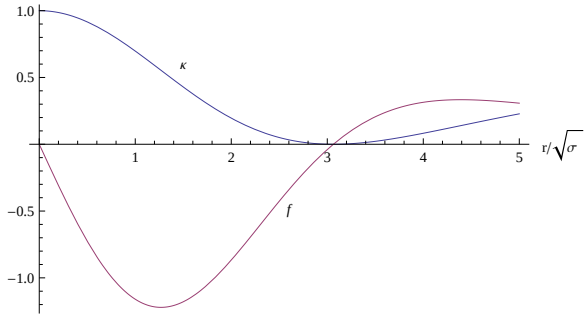

Figure 4.12: A plot of the metric function f and surface gravity κ for $M = 1.85579\sqrt{\theta}$, and $Q = M/2$.

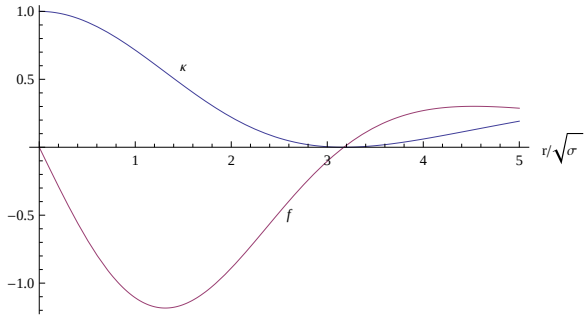

Figure 4.13: A plot of the metric function f and κ for $M = 1.7318\sqrt{\theta}$, and $Q = M$.

single solution to equation 4.40, namely $r = M = Q$. Since there is no restriction on the relation between Q and M, we begin with a choice of $Q = \alpha M$, for some α not necessarily less than 1. We then simultaneously solve the pair of equations $f = 0$ and $\kappa = 0$ and obtain numerical results. These are presented in Table 4.1, with selected Q/M-ratios in Figures 4.12,4.13,4.14, as well as in Figure 4.15.

We now summarize these results. It is evident from these plots that for a larger $Q = \alpha M$, even $Q > M$, the minimum mass necessary to ensure an apparent horizon becomes less. This is as expected, considering our earlier observation that an electric charge in a noncommutative Reissner-Nordström black hole acts as a matter field. It also seems from Figure 4.16 that for a larger charge, there is a maximum size for the initial formation of the apparent horizon. We plot this in Figure 4.17 for a physically-unreasonable $Q = 30000M$. At this choice of Q, we have the approximate solution

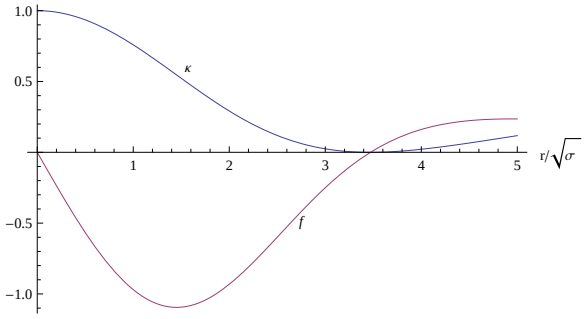

Figure 4.14: A plot of the metric function f and κ for $M = 1.41591\sqrt{\theta}$, and $Q = 2M$.

α $(Q = \alpha M)$	$M/\sqrt{\theta}$	$r_H/\sqrt{\theta}$
0.	1.90412	3.02244
0.25	1.89165	3.03295
0.5	1.85579	3.06347
0.75	1.80067	3.11121
1.	1.7318	3.17226
1.25	1.65476	3.24236
1.5	1.57426	3.31759
1.75	1.49386	3.3947
2.	1.41591	3.47126

Table 4.1: Extremal solutions for noncommutative Reissner-Nordström black holes

$(Q, M, r) \approx (5.01\sqrt{\theta}, 0.0002\sqrt{\theta}, 5.01\sqrt{\theta})$. For $Q/M \gg 1$, we have the "maximally extremal" $M = 0$ and $r_H = Q \approx 5\sqrt{\theta}$.

Alternatively, the surface gravity on the horizon of a stationary spherically-symmetric black hole satisfies the relation [9]

$$\mathscr{L}_\ell \theta_{(n)} + \kappa\theta_{(n)} + \frac{\tilde{R}}{2} = \tilde{d}\tilde{\omega}^a + \tilde{\omega}^a\tilde{\omega}_a + 8\pi G T_{ab}\ell^a n^b \tag{4.41}$$

where the tilde represents measures on the horizon 2-surface; as well, $\theta_{(n)}$ is the inward

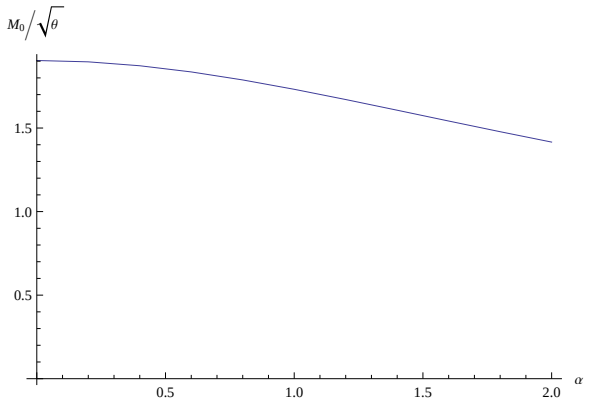

Figure 4.15: Minimal mass for Reissner-Nordström solution compared to charge $Q = \alpha M$.

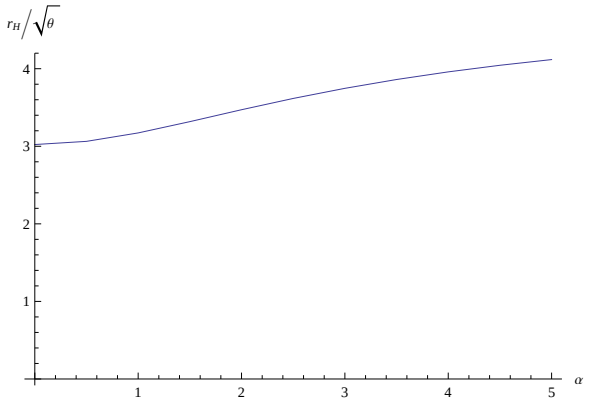

Figure 4.16: Horizon size for extremal Reissner-Nordström black hole with charge $Q = \alpha M$.

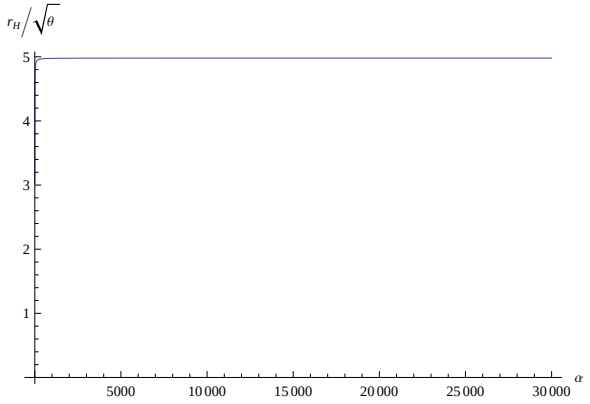

Figure 4.17: Horizon size for extremal Reissner-Nordström black hole with very large charge $Q = \alpha M$.

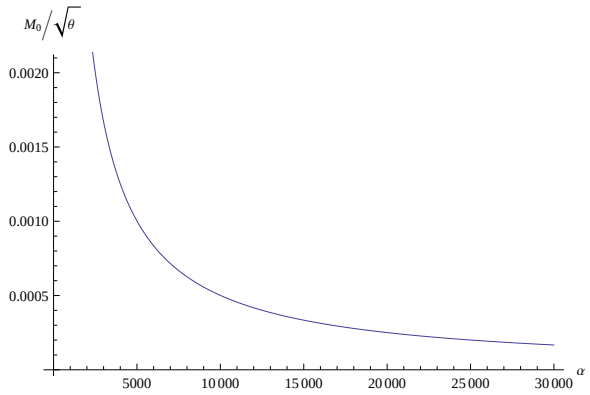

Figure 4.18: Minimal mass for extremal Reissner-Nordström black hole with very large charge $Q = \alpha M$.

expansion of the horizon, ℓ^a and n^a are null vectors, $\tilde{R}$ is the scalar curvature of the horizon, $\tilde{\omega}^a$ is the angular momentum one-form and $\tilde{d}$ is the derivative operator on the surface. In our context, we have $\mathscr{L}_\ell \theta_{(n)} = 0$, $\tilde{\omega}^a = 0$, and $\tilde{R} = 2/r^2$ on the horizon sphere. We use $\ell^a = \frac{-f}{2}\delta^a_0 - \delta^a_1$ and $n^a = \delta^a_0$ as our null vectors. The inward expansion of the horizon is

$$\theta_{(n)} = \tilde{q}^{ab} n_{b;a} = -\frac{2}{r} \tag{4.42}$$

and so equation 4.41 gives

$$\frac{-2\kappa}{r} + \frac{2/r^2}{2} = \frac{1 - f - rf'}{r^2} \tag{4.43}$$

Solving for κ, we obtain

$$\kappa = \frac{f + rf'}{2r} \tag{4.44}$$

For an extremal black hole, $\kappa = 0$ implies that $f + rf' = 0$. We already know that on the horizon of any black hole $f = 0$. Further, recall that the extremal locus (v, r) is a minimum of the apparent-horizon-curve in Figure 4.2. At such a point, $f' = 0$.

In summary, in a charged, noncommutative solution, there is no restriction on charge and mass. Varied solutions are possible, including a "maximally-extremal", massless

black hole. In a noncommutative Reissner-Nordström solution, the charge parameter contributes non-trivially to the mass of the black hole, making this massless solution possible. Further, for a larger charge a smaller mass is required to ensure existence of the apparent horizon. Regardless of charge-to-mass ratio, the horizon exists at a larger radius than the Schwarzschild case, with $3 \leq r_H/\sqrt{\theta} \leq 5$.

If indeed it is possible for a black hole to form with $Q > M$, we would expect that in the commutative (classical) limit, that charge would somehow be lost as mass accretes to ensure $M \geq Q$. This transition however, is not yet described, as the current noncommutative model does not allow for large masses, which we have already shown.

4.2.2 Dynamic correspondence

We have shown that the existence of the apparent horizon for a noncommutative black hole is unconstrained by its charge-versus-mass ratio. Generally, a noncommutative solution has two horizons for sufficiently-large choices of mass and charge. There exists a critical point at which only a single horizon exists, and we have called this point extremal.

If we now compare the previous result to a dynamic solution, we can make a correspondence between the two. The result is that a choice of parameters for M and Q have dual purpose. Solving $f(r) = 0$ and $\kappa(r) = 0$ provides a set of parameters (M, Q, r_H) that denote a static extremal horizon, but *also* satisfy the location of the formation of the apparent horizon at an earliest-possible time in v for an equivalent dynamic solution.

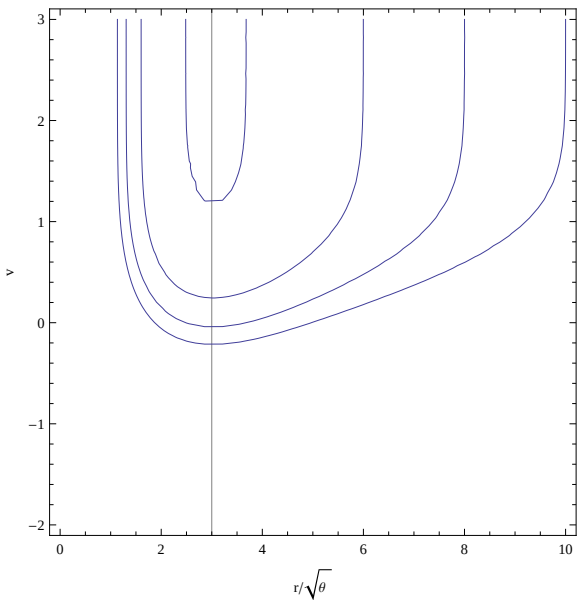

Figure 4.19: Horizons for varying masses of a noncommutative uncharged Vaidya black hole, showing that the initial areal radius of the black hole is independent of mass. From top to bottom, $M/\sqrt{\theta} \in \{2, 3, 4, 5\}$.

We begin first with the noncommutative Schwarzschild-Vaidya, which exhibits an "extremal" state at $r \approx 3\sqrt{\theta}$ for any choice of mass. This seems strange, yet provides an interesting insight in a dynamic form of this metric.

Analogously, in a dynamic Schwarzschild spacetime (i.e., the uncharged Vaidya solution), the moment of formation of the apparent horizon is fixed at about $r \approx 3\sqrt{\theta}$, regardless of mass accretion. For a smaller final mass, the apparent horizon will form *later* so as to have accumulated sufficient mass to form the horizon. For a larger final mass, the apparent horizon will form earlier. This is evident in Figure 4.19. In that figure, the minimum point of that curve at $r \approx 3\sqrt{\theta}$ corresponds to both the extremal state of a static black hole, as well as the moment of formation of the apparent horizon. We are evaluating that "moment" in v as a state, at which the spacetime is, in some sense, static.

In the noncommutative charged Vaidya black hole, we have an extra parameter, Q,

that traditionally represents the charge, but also contributes to the perceived matter field. We then have a 4-parameter space, (v, M, Q, r) where we search for a point in v at which the apparent horizon forms. The extremal horizon in a static black hole is located at a locus (M, Q, r_H) which corresponds to a point (v, M, Q, r_H). This is the minimum of the curve shown in Figures 4.20,4.21,4.22. For any dynamic, charged, noncommutative black hole, the apparent horizon forms at a point (v, r) that is tangent to an ingoing null ray: this is the minimum point in Figures 4.20,4.21,4.22. This point is equivalent to the extremal horizon for a static black hole with the same parameter choice of M and Q.

While extremality and surface gravity do not directly apply to a dynamic solution, we see that there is a useful correspondence. We can use a static form of a black hole to determine extremality via the surface gravity, and use the resulting solution as a parameter choice for a dynamic solution. This resulting solution corresponds to the single apparent horizon that forms at the earliest possible time v, where after the horizon bifurcates.

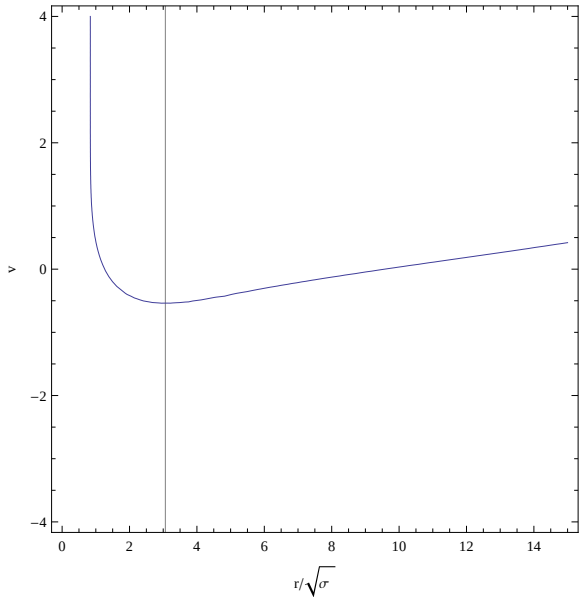

Figure 4.20: Horizon for the charged Vaidya solution, with the location of the apparent horizon at formation shown, for $M = 1.85579\sqrt{\theta}$ and $Q = M/2$.

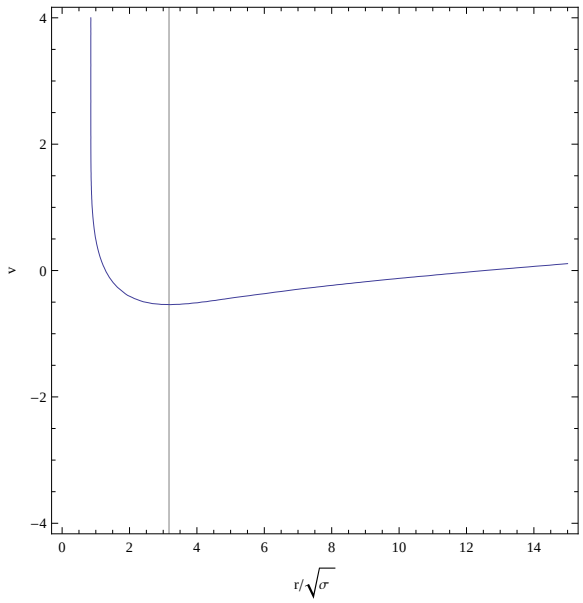

Figure 4.21: Horizon for the charged Vaidya solution, with the location of the apparent horizon at formation shown, for $M = 1.7318\sqrt{\theta}$ and $Q = M$.

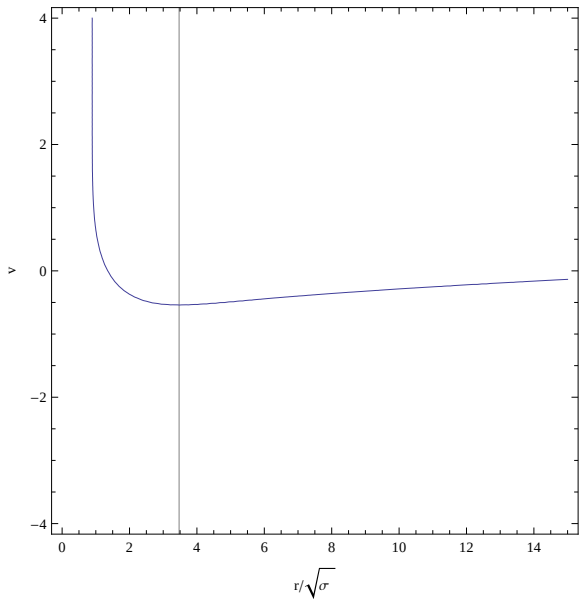

Figure 4.22: Horizon for the charged Vaidya solution, with the location of the apparent horizon at formation shown, for $M = 1.41591\sqrt{\theta}$ and $Q = 2M$.

Chapter 5

Alternate noncommutative solution

In this section we consider the energy conditions in the context of a noncommutative spacetime. We begin with the calculation of a stress-energy tensor. We use a particular expansion of the stress-energy tensor along null normals to the black hole horizon. This allows us to consider the energy-condition requirements on a general dynamic spacetime. It becomes quite obvious that the addition of noncommutativity breaks the energy conditions in various ways. These violations are indeed serious, as nothing out-of-the-ordinary has been done to these models: they are the most basic models, differing from classical models in only the noncommutativity. We then propose a new noncommutative solution that satisfies the energy conditions. We impose an equation of state that defines a relation between pressure and density. The non-violating solution also encompasses a set of solutions with some freedom of choice in parameters.

5.1 Energy conditions

It is possible to create strange and physically-unrealistic spacetimes that still satisfy Einstein's equations. In order to maintain some reasonable expectations on how a spacetime should behave, the energy conditions provide restrictions that ensure things such as negative energy densities, closed timelike curves, and naked singularities do not exist.

The failure of a noncommutative spacetime to satisfy the energy conditions has already been discussed briefly [30]; in summary, the energy conditions (weak, strong, dominant) generally fail in the region $r < 6\sqrt{\theta}$. Classically, this would be acceptable as this value is incredibly close to the singularity, where strong quantum gravity effects would be expected. We present here some more detailed calculations of the stress-energy tensor, in light of the energy conditions.

Often, the stress-energy tensor is considered in an orthonormal basis e^{μ}_{α}, where it has the decomposition,

$$T^{\alpha\beta} = p^i e^{\alpha}_i e^{\beta}_i, \tag{5.1}$$

for some values p^i, $i = 0, \ldots, 3$.

We show below the calculations of Wong & Wu [51] that produce a decomposition of the stress-energy tensor for a Vaidya spacetime. Note that the mass function used is $m(v, r)$; this means that their results can be equally applied to a noncommutative metric where mass (and charge) are independent on r. Assume Eddington-Finkelstein null coordinates, with a metric function of $f(v, r) = 1 - \frac{2m(v,r)}{r}$. Define then two null vectors, $\ell_\mu = \delta^0_\mu$ and $n_\mu = \frac{1}{2}\left(1 - \frac{2m(v,r)}{r}\right)\delta^0_\mu - \delta^1_\mu$, that are also cross-normalized: $\ell_\mu n^\mu = -1$.

Calculating the stress energy tensor from $G_{\alpha\beta} = 8\pi T_{\alpha\beta}$, one obtains

$$T_{vv} = \rho\left(1 - \frac{2m}{r}\right) + \frac{\dot{m}}{4\pi r^2} \tag{5.2}$$

$$T_{vr} = -\rho \tag{5.3}$$

$$T_{\theta\theta} = P g_{\theta\theta} \tag{5.4}$$

$$T_{\phi\phi} = P g_{\phi\phi} \tag{5.5}$$

where

$$\rho = -\frac{m'}{4\pi r^2} \tag{5.6}$$

$$P = -\frac{m''}{8\pi r} \tag{5.7}$$

Note that the over-dot represents a derivative with respect to v, and the prime represents a derivative with respect to r.

Using the two null vectors ℓ_μ and n_μ, the stress-energy tensor can be written

$$T_{\alpha\beta} = \frac{\dot{m}}{4\pi r^2}\ell_\alpha \ell_\beta + \rho\left(\ell_\alpha n_\beta + \ell_\beta n_\alpha\right) + P(g_{\alpha\beta} + \ell_\alpha n_\beta + \ell_\beta n_\alpha) \tag{5.8}$$

Note that $T_{\alpha\beta} n^\alpha n^\beta = \frac{\dot{m}}{4\pi r^2}$, whereas $T_{\alpha\beta}\ell^\alpha \ell^\beta = 0$; there is energy flux along n^α only. Defining

$$\mu(v, r) = \frac{\dot{m}}{4\pi r^2}, \tag{5.9}$$

the tensor can be written in terms of these two vectors:

$$T_{\alpha\beta} = T^{(n)}_{\alpha\beta} + T^{(m)}_{\alpha\beta} \tag{5.10}$$

where

$$T^{(n)}_{\alpha\beta} = \mu \ell_\alpha \ell_\beta \tag{5.11}$$

$$T^{(m)}_{\alpha\beta} = (\rho + P)(\ell_\alpha n_\beta + \ell_\beta n_\alpha) + P g_{\alpha\beta} \tag{5.12}$$

The case where $P = \rho = 0$ leaves only $T_{vv} = \frac{\dot{m}}{4\pi r^2}$, which is the only non-zero component of the tensor for the non-charged Vaidya solution.

Using the orthonormal basis

$$e^\mu_0 = \frac{\ell^\mu + n^\mu}{\sqrt{2}} \tag{5.13}$$

$$e^\mu_1 = \frac{\ell^\mu - n^\mu}{\sqrt{2}} \tag{5.14}$$

$$e^\mu_2 = \frac{1}{r}\delta^\mu_\theta \tag{5.15}$$

$$e^\mu_3 = \frac{1}{r\sin(\theta)}\delta^\mu_\phi, \tag{5.16}$$

the tensor takes the form

$$T_{\hat{\alpha}\hat{\beta}} = \begin{pmatrix} \frac{\mu}{2} + \rho & \frac{\mu}{2} & 0 & 0 \\ \frac{\mu}{2} & \frac{\mu}{2} - \rho & 0 & 0 \\ 0 & 0 & P & 0 \\ 0 & 0 & 0 & P \end{pmatrix}. \tag{5.17}$$

Using the (μ, ρ, P) decomposition, we have the following forms of the energy conditions, described in [51]:

Weak and strong: $\mu \geq 0, \rho \geq 0, P \geq 0$

Dominant: $\mu \geq 0, \rho \geq P \geq 0$

This formulation is easily extended to the generalized noncommutative solution, if we consider $M(v,r)$ as encompassing all parameters, the metric function becomes

$$1 - \frac{2M(v,r)}{r} = 1 - \frac{2}{r}\left(\frac{2m(v)}{\sqrt{\pi}}\gamma\left(\frac{3}{2}, \frac{r^2}{4\theta}\right) - \frac{q(v)^2}{2\pi r}\left(\gamma\left(\frac{1}{2}, \frac{r^2}{4\theta}\right)^2 - \frac{r}{\sqrt{2\theta}}\gamma\left(\frac{1}{2}, \frac{r^2}{2\theta}\right)\right)\right). \tag{5.18}$$

Before examining the noncommutative behaviour, we first discuss any issues created by the time-dependence of the metric. Any static solution has $\mu = 0$; there are conditions on dynamic solutions. In a non-charged case, the requirement is simply that $\dot{m} \geq 0$. In a charged case, the requirement is that $r\dot{m}(v) - q(v)\dot{Q}(v) \geq 0$. Since $m(v)$ and $q(v)$ are proportional (both functions of $\mathcal{E}(v)$), then this reduces to $r \geq \frac{q_f}{m_f} q(v)$. For $q(v) \in (0, q_f)$, we have $r \geq \frac{q_f^2}{m_f}$ in the limit as $v \to \infty$. The region of violation is $r < \frac{q_f^2}{m_f} \leq m_f$, since $q_f \leq m_f$. In the classically extremal case, $m_f = q_f$, and the region is the entire interior of the black hole, since $r = \frac{m_f^2}{m_f} = m_f$ is the horizon. In a classically non-extremal case, it appears that there is a region $r \leq \frac{q_f^2}{m_f} < m_f$ which still breaks the energy conditions.

In the most general *classical* case, then, we have the requirements $\dot{m}(v) \geq 0$, and, at late times, $\frac{q_f^2}{m_f} \leq r$.

Table 5.1: Energy-condition restrictions on classical spacetimes

	$8\pi\mu$	$8\pi\rho$	$8\pi P$	Restrictions
Schw.	0	0	0	Satisfied everywhere
Vaidya	$2\dot{m}/r^2$	0	0	$\dot{m} \geq 0$
R-N	0	Q^2/r^4	Q^2/r^4	Satisfied everywhere
Vaidya R-N	$2\left(r\dot{m} - q\,\dot{q}\right)/r^3$	q^2/r^4	q^2/r^4	$r\dot{m} - q\,\dot{q} \geq 0$

The charged Vaidya condition $r\dot{m} - q\,\dot{q} \geq 0$ can be satisfied under the following assumptions.
If $m(v)$ and $q(v)$ are proportional — $m(v) = m\mathcal{F}(v)$ and $q(v) = q\mathcal{F}(v)$ — then $\dot{q}/\dot{m} = q/m$, and then $r \geq q^2/m$.

We present in Table 5.1 the classical energy conditions, and below the calculated μ, ρ, and P for the noncommutative spacetimes. Where possible, we show the energy conditions' restrictions on those functions.

Schwarzschild

$$\begin{aligned} 8\pi\mu &= 0 \\ 8\pi\rho &= \frac{\mathrm{e}^{-\frac{r^2}{4\theta}} m}{\sqrt{\pi}\theta^{3/2}} \\ 8\pi P &= \frac{\mathrm{e}^{-\frac{r^2}{4\theta}} \left(r^2 - 4\theta\right) m}{4\sqrt{\pi}\theta^{5/2}} \end{aligned} \tag{5.19}$$

Weak & Strong: $2 \leq \frac{r}{\sqrt{\theta}}$

Dominant: $2 \leq \frac{r}{\sqrt{\theta}} \leq \sqrt{8}$

Vaidya

$$
\begin{aligned}
8\pi\mu &= \frac{4\gamma\left(\frac{3}{2},\frac{r^2}{4\theta}\right)\dot{m}(v)}{\sqrt{\pi}r^2} \\
8\pi\rho &= \frac{\mathrm{e}^{-\frac{r^2}{4\theta}}m}{\sqrt{\pi}\theta^{3/2}} \\
8\pi P &= \frac{\mathrm{e}^{-\frac{r^2}{4\theta}}\left(r^2-4\theta\right)m}{4\sqrt{\pi}\theta^{5/2}}
\end{aligned}
\tag{5.20}
$$

Weak & Strong: $\dot{m}(v) \geq 0;\ 2 \leq \frac{r}{\sqrt{\theta}}$

Dominant: $\dot{m}(v) \geq 0;\ 2 \leq \frac{r}{\sqrt{\theta}} \leq \sqrt{8}$

Reissner-Nordström

$$
\begin{aligned}
8\pi\mu &= 0 \\
8\pi\rho &= \frac{\mathrm{e}^{-\frac{r^2}{2\theta}}Q^2}{\pi\theta r^2} + \frac{Q^2}{r^4}\left(\mathcal{E}\left(\frac{r}{2\sqrt{\theta}}\right)\right)^2 + \frac{\mathrm{e}^{-\frac{r^2}{4\theta}}\left(mr^3 - 2Q^2\theta\,\mathcal{E}\left(\frac{r}{2\sqrt{\theta}}\right)\right)}{\sqrt{\pi}\theta^{3/2}r^3} \\
8\pi P &= \frac{1}{4\pi r^4\theta^{5/2}}\mathrm{e}^{-\frac{r^2}{2\theta}}\left(2Q^2r^2\sqrt{\theta}\left(r^2+2\theta\right) + 4\mathrm{e}^{\frac{r^2}{2\theta}}\pi Q^2\theta^{5/2}\left(\mathcal{E}\left(\frac{r}{2\sqrt{\theta}}\right)\right)^2\right. \\
&\qquad \left. +\mathrm{e}^{\frac{r^2}{4\theta}}\sqrt{\pi}r\left(mr^3(r^2-4\theta) - 2Q^2\theta(r^2+4\theta)\,\mathcal{E}\left(\frac{r}{2\sqrt{\theta}}\right)\right)\right)
\end{aligned}
\tag{5.21}
$$

Charged Vaidya

$$
\begin{aligned}
8\pi\mu &= \frac{1}{\pi r^3}\left(4\sqrt{\pi}r\gamma\left(\frac{3}{2},\frac{r^2}{4\theta}\right)\dot{m}(v)+\left(-2\pi\left(\mathcal{E}\left(\frac{r}{2\sqrt{\theta}}\right)\right)^2+\frac{\sqrt{2\pi}r\,\mathcal{E}\left(\frac{r}{\sqrt{2\theta}}\right)}{\sqrt{\theta}}\right)q(v)\dot{Q}(v)\right)\\
8\pi\rho &= \frac{1}{\pi r^4\theta^{3/2}}\mathrm{e}^{-\frac{r^2}{2\theta}}\left(\mathrm{e}^{\frac{r^2}{4\theta}}\sqrt{\pi}r^4m(v)+\sqrt{\theta}\left(r-\mathrm{e}^{\frac{r^2}{4\theta}}\sqrt{\theta}\gamma\left(\frac{1}{2},\frac{r^2}{4\theta}\right)\right)^2q(v)^2\right)
\end{aligned}
\tag{5.22}
$$

$$
\begin{aligned}
8\pi P = \frac{1}{4\pi r^4\theta^{5/2}}\mathrm{e}^{-\frac{r^2}{2\theta}}\Bigg(&2r^2\sqrt{\theta}\left(r^2+2\theta\right)q(v)^2+4\mathrm{e}^{\frac{r^2}{2\theta}}\pi\theta^{5/2}\,\mathcal{E}\left(\frac{r}{2\sqrt{\theta}}\right)^2q(v)^2\\
&+\mathrm{e}^{\frac{r^2}{4\theta}}\sqrt{\pi}r\left(\left(r^5-4r^3\theta\right)m(v)-2\theta\left(r^2+4\theta\right)\mathcal{E}\left(\frac{r}{2\sqrt{\theta}}\right)q(v)^2\right)\Bigg)
\end{aligned}
$$

5.1.1 Energy-condition analysis: noncommutative Reissner-Nordström

A simple case to begin with is a (static) noncommutative Reissner-Nordström. The calculated μ, ρ, and P are:

$$
\begin{aligned}
8\pi\mu &= 0\\
8\pi\rho &= \frac{\mathrm{e}^{-\frac{r^2}{2\theta}}Q^2}{\pi\theta r^2}+\frac{Q^2}{r^4}\left(\mathcal{E}\left(\frac{r}{2\sqrt{\theta}}\right)\right)^2+\frac{\mathrm{e}^{-\frac{r^2}{4\theta}}\left(Mr^3-2Q^2\theta\,\mathcal{E}\left(\frac{r}{2\sqrt{\theta}}\right)\right)}{\sqrt{\pi}\theta^{3/2}r^3}\\
&\quad+\mathrm{e}^{\frac{r^2}{4\theta}}\sqrt{\pi}r\left(Mr^3(r^2-4\theta)-2Q^2\theta(r^2+4\theta)\,\mathcal{E}\left(\frac{r}{2\sqrt{\theta}}\right)\right)\Bigg)\\
8\pi P &= \frac{1}{4\pi r^4\theta^{5/2}}\mathrm{e}^{-\frac{r^2}{2\theta}}\left(2Q^2r^2\sqrt{\theta}\left(r^2+2\theta\right)+4\mathrm{e}^{\frac{r^2}{2\theta}}\pi Q^2\theta^{5/2}\left(\mathcal{E}\left(\frac{r}{2\sqrt{\theta}}\right)\right)^2\right.
\end{aligned}
\tag{5.23}
$$

We begin with some numerical comparison of the behaviour of ρ and P. Their limiting

values are, for ρ,

$$\lim_{r\to 0}\rho = \frac{M}{\sqrt{\pi}\theta^{3/2}} \tag{5.24}$$

$$\lim_{r\to\infty}\rho = 0, \tag{5.25}$$

and for P,

$$\lim_{r\to 0}P = -\frac{M}{\sqrt{\pi}\theta^{3/2}} \tag{5.26}$$

$$\lim_{r\to\infty}P = 0. \tag{5.27}$$

Initially, $P < 0$ is a problem, which breaks the weak and strong conditions. The weak and strong require that $\rho \geq 0$ and $P \geq 0$. This is always true for ρ, but P changes value at approximately $r = 0.45$, based on Figure 5.1.

Further, the dominant energy condition is satisfied for r up to a particular point r_c, where $\rho(r_c) = P(r_c)$, as shown in Figures 5.1, 5.2, 5.3. It would appear that as Q/M grows beyond unity, then the limit of $(\rho - P)(r)$ is positive everywhere; however, this is not the case. There remains a region (r_c, ∞) where the dominant condition fails. This is evidenced in Figure 5.4.

We should reasonably expect that a noncommutative black hole will smoothly grow into a commutative one. With that expectation, we could expect some restriction on Q so that $Q > M$ is forbidden as M and Q grow. The classical conditions are satisfied everywhere, yet the noncommutative solution creates many regions in r where the conditions are not satisfied.

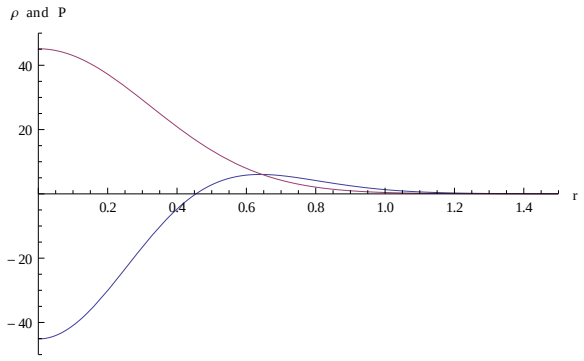

Figure 5.1: A combined graph of $\rho(r)$ and $P(r)$ for a noncommutative Reissner-Nordström black hole. ($M = 4\sqrt{\theta}$, $Q = 0.4M$)

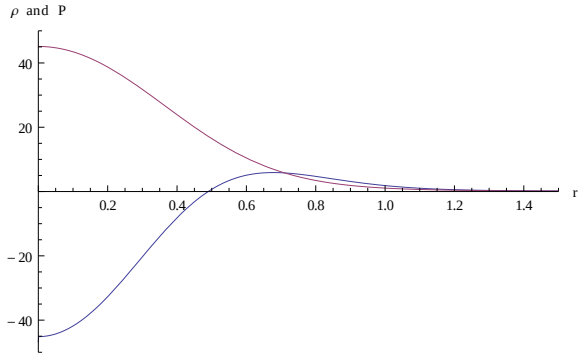

Figure 5.2: A combined graph of $\rho(r)$ and $P(r)$ for a noncommutative Reissner-Nordström black hole. ($M = 4\sqrt{\theta}$, $Q = M$)

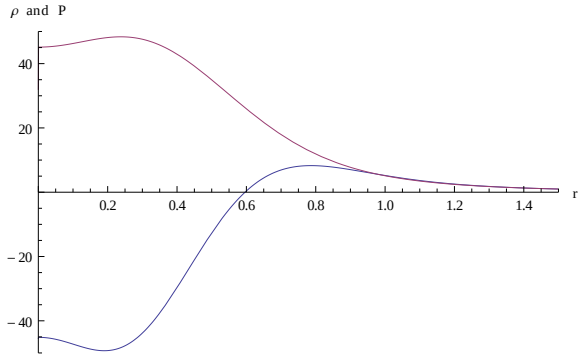

Figure 5.3: A combined graph of $\rho(r)$ and $P(r)$ for a noncommutative Reissner-Nordström black hole. ($M = 4\sqrt{\theta}$, $Q = 2.5M$)

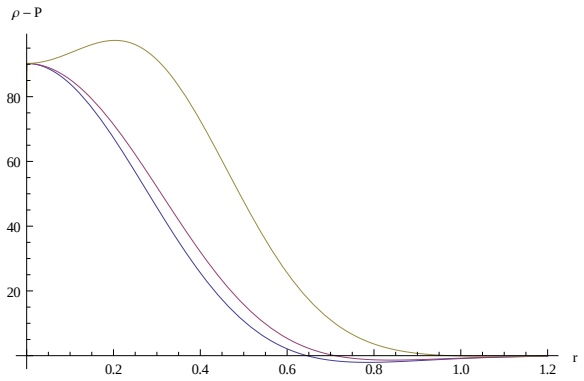

Figure 5.4: A graph of $(\rho - P)(r)$for a noncommutative Reissner-Nordström black hole. From top to bottom, $Q = 2.5M$, $Q = M$, $Q = 0.4M$.

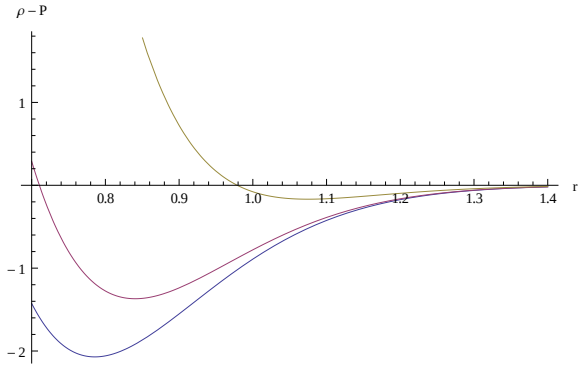

Figure 5.5: A restricted view of 5.4.

5.2 Choice of fluids

We now derive a noncommutative solution that satisfies the energy conditions. We begin with some comments on the nature of the noncommutative Schwarzschild-Vaidya black hole. The metric function is

$$f(v,r) = 1 - \frac{4m(v)}{\sqrt{\pi}r}\gamma\left(\frac{3}{2}, \frac{r^2}{4\theta}\right), \tag{5.28}$$

which leads to a stress energy tensor of

$$T^{\alpha}{}_{\beta} = \begin{pmatrix} -\frac{e^{-\frac{r^2}{4\theta}} m(v)}{\sqrt{\pi}\theta^{3/2}} & 0 & 0 & 0 \\ \frac{4\gamma\left(\frac{3}{2},\frac{r^2}{4\theta}\right)\dot{m}(v)}{\sqrt{\pi}r^2} & -\frac{e^{-\frac{r^2}{4\theta}} m(v)}{\sqrt{\pi}\theta^{3/2}} & 0 & 0 \\ 0 & 0 & \frac{e^{-\frac{r^2}{4\theta}}(r^2-4\theta)m(v)}{4\sqrt{\pi}\theta^{5/2}} & 0 \\ 0 & 0 & 0 & \frac{e^{-\frac{r^2}{4\theta}}(r^2-4\theta)m(v)}{4\sqrt{\pi}\theta^{5/2}} \end{pmatrix}. \tag{5.29}$$

The density, $-\rho \equiv T^{v}{}_{v}$, is

$$\rho = \frac{e^{-\frac{r^2}{4\theta}} m(v)}{\sqrt{\pi}\theta^{3/2}}. \tag{5.30}$$

For any given r, the density is of course proportional to the mass, with a maximum at $r = 0$. At large r the density becomes negligible.

The pressure, $P \equiv T^{\vartheta}{}_{\vartheta} = T^{\phi}{}_{\phi}$, is

$$P = \frac{e^{-\frac{r^2}{4\theta}}(r^2 - 4\theta)m(v)}{4\sqrt{\pi}\theta^{5/2}}. \tag{5.31}$$

The pressure varies with r more so than the density; refer to Figure 5.6, where m

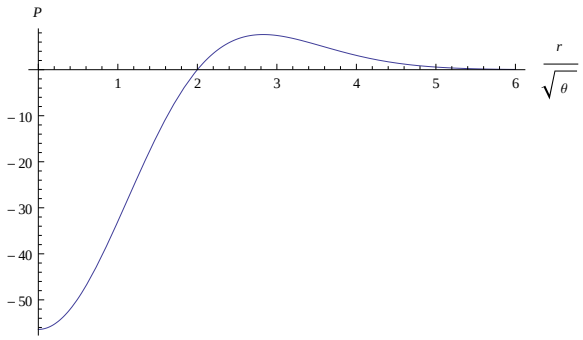

Figure 5.6: Pressure of a noncommutative Schwarzschild black hole.

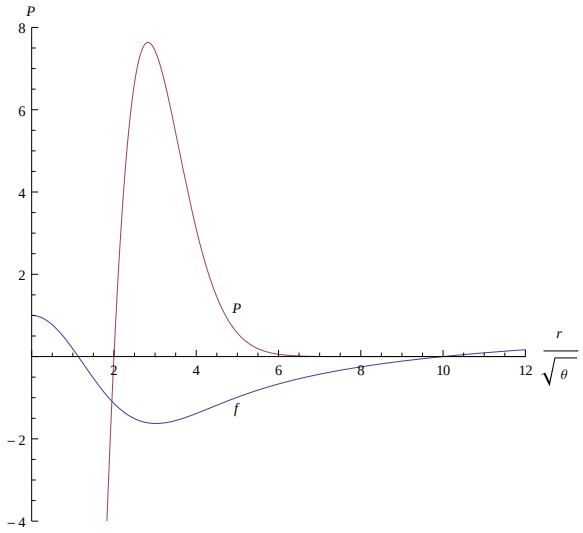

Figure 5.7: Pressure of a noncommutative Schwarzschild black hole as compared to its horizons.

is taken at its maximum. We see that the pressure changes sign at $r = 2\sqrt{\theta}$, from negative to positive. Refer as well to Figure 5.7 to see that this root does not correspond to the horizons in any way. We see however, that outside the black hole, the pressure is asymptotically zero. Inside, we have a stranger picture, in that the pressure is negative inside the inner Cauchy horizon, and outside up to some r, at which point the pressure becomes positive.

It is possible to find different spacetime solutions based on fluid choice. The Vaidya solution is usually considered in the context of null fluid collapse. Other solutions

have been found in anisotropic space [26, 45], where

$$T^{\alpha}{}_{\beta} = (-\rho, p_r, p_\perp, p_\perp) \tag{5.32}$$

where the conservation law $T^{\alpha\beta}{}_{;\beta} = 0$ requires

$$\begin{aligned} p_r &= -\rho \\ p_\perp &= -\rho - r\partial_r\rho \end{aligned} \tag{5.33}$$

For the noncommutative Schwarzschild-Vaidya black hole, note that the pressure and density are related by a factor of

$$\frac{P}{\rho} = -\left(\frac{r^2}{4\theta} - 1\right). \tag{5.34}$$

This is equivalent to $p_\perp = -\rho - \frac{r}{2}\partial_r\rho$, which is anisotropic. Anisotropic spaces are direction-dependent. Compare that to an *isotropic* or *perfect* fluid in which the fluid is identical in all directions. Other possible fluids include *null dusts*, which are pressureless. This is found in the classical Vaidya solution, which has a stress-energy tensor with $T_{00} = -\dot{m}(v)/4\pi r^2$ as the only non-zero component. This represents the energy density, and so there is no pressure. Matter fields of strange quark matter have also been considered, where there is an equation of state $P = \frac{1}{3}(\rho - 4B)$, where B is the bag constant (the difference between the energy density of the perturbative and non-perturbative QCD vacuum) [21]. This equation of state resembles the state we will choose below.

In following the work of V. Husain in [23], we instead impose the perfect fluid require-

ment

$$P = k\rho^a \tag{5.35}$$

for some k and a to be determined later so as to ensure compliance with the dominant energy condition, $\rho \geq P \geq 0$. This resembles a polytropic fluid, where classical polytropes have $a \equiv (n+1)/n > 1$ for $n \in \mathbb{Z}$.

Husain showed that $k = \frac{1}{2}$ is a critical value for the asymptotic behaviour of the spacetime. For $0 < k < \frac{1}{2}$, the spacetime was cosmological; for $\frac{1}{2} < k \leq 1$, the spacetime was asymptotically flat. The value $k = \frac{1}{2}$ was not considered, as neither the weak nor dominant conditions could be satisfied.

Our solution is found as follows. First, choose a generic metric function

$$f(v, r) = 1 - \frac{2M(v, r)}{r} \tag{5.36}$$

in an Eddington-Finkelstein-type metric

$$ds^2 = -f(v, r)dv^2 + 2dvdr + r^2 d\vartheta^2 + r^2 \sin^2(\vartheta)d\phi. \tag{5.37}$$

We calculate the stress-energy tensor, and impose our requirement of $P = k\rho^a$. Given that $T^v{}_v = -\rho$ and $T^\phi{}_\phi = P$, we have the equation

$$G^v{}_v + G^\phi{}_\phi = 8\pi \left(k\rho^a - \rho\right) \tag{5.38}$$

which is the PDE

$$-\frac{2M'(v, r) + rM''(v, r)}{r^2} = 8\pi \left(k\rho^a - \rho\right). \tag{5.39}$$

To ensure noncommutativity, we assume a matter density of

$$\rho(v,r) = \frac{m(v)}{(4\pi\theta)^{3/2}} \mathrm{e}^{-\frac{r^2}{4\theta}}. \tag{5.40}$$

Solving the PDE, we find

$$\begin{aligned} M(v,r) = 2 &\left(\frac{4\mathrm{e}^{-\frac{r^2}{4\theta}}\sqrt{\theta}}{\sqrt{\pi}r} + \mathcal{E}\left(\frac{r}{2\sqrt{\theta}}\right)\right) m(v) \\ &- \frac{2^{4-3a}\pi^{1-\frac{3a}{2}}\theta^{3(1-a)/2}k\mathrm{e}^{-\frac{ar^2}{4\theta}}\left(4\sqrt{\theta} + \sqrt{a}\mathrm{e}^{\frac{ar^2}{4\theta}}\sqrt{\pi}r\,\mathcal{E}\left(\frac{\sqrt{a}r}{2\sqrt{\theta}}\right)\right) m^a(v)}{a^2 r} \\ &- \frac{C_1(v)}{r} + C_2(v) \end{aligned} \tag{5.41}$$

where $C_1(v)$ and $C_2(v)$ are arbitrary functions of integration. We choose $C_2(v) = 0$ so that in the limit $r/\sqrt{\theta} \to \infty$, $M(v,r) \to m(v)$.

We must now be careful with our parameter choice. Note first that for any choices of a and k, $\rho \geq 0$ and $P \geq 0$, and so both the weak and strong conditions are satisfied. However, the dominant condition requires more careful consideration. We consider the following choices, with justifications to follow:

- $k = 0$
- $0 \leq a < 1 \implies k = 0$;
- $a = 1 \implies k \leq 1$;
- $a \equiv 1 + \frac{1}{n}, n \in \mathbb{Z} \implies k\rho^{\frac{1}{n}} \leq 1$.

Setting $k = 0$ we have the following noncommutative-like function, independent of a. Note, then, that we are *free to choose* $k = 0$ *first* without any restriction on a.

$$M(v,r) = 2\left(\frac{4\mathrm{e}^{-\frac{r^2}{4\theta}}\sqrt{\theta}}{\sqrt{\pi}r} + \mathcal{E}\left(\frac{r}{2\sqrt{\theta}}\right)\right)m(v) - \frac{C_1(v)}{r}. \tag{5.42}$$

The metric would then read

$$f(v,r) = 1 - \frac{4m(v)}{r}\left(\frac{4\mathrm{e}^{-\frac{r^2}{4\theta}}\sqrt{\theta}}{\sqrt{\pi}r} + \mathcal{E}\left(\frac{r}{2\sqrt{\theta}}\right)\right) + \frac{2\sqrt{\pi}C_1(v) - 16\mathrm{e}^{-\frac{r^2}{4\theta}}\sqrt{\theta}m(v)}{\sqrt{\pi}r^2}. \tag{5.43}$$

Rather than choose $C_1(v) = 0$ as suggested above, we may rather want to have $C_1(v)$ be a limit on the charge term so that $2\sqrt{\pi}C_1(v) - 16\mathrm{e}^{-\frac{r^2}{4\theta}}\sqrt{\theta}m(v) > 0$. Considering that $\mathrm{e}^{-\frac{r^2}{4\theta}}$ has a maximum at $r = 0$, the requirement on $C_1(v)$ is

$$C_1(v) > 8\sqrt{\frac{\theta}{\pi}}m(v). \tag{5.44}$$

This would then ensure that the effective charge is positive.

Consider Figure 5.8, with varying choices of $C_1(v)$. We see that for $C_1(v) = c\sqrt{\frac{\theta}{\pi}}m(v)$, the horizon behaviour changes at $c = 8$. For $c < 8$, there is a single horizon, for $c > 8$ there are two. In the left-hand limit $c \to 8^-$, there are at most three horizons. One could consider this a point of extremality. As c grows up to $c = 8$, the inner most horizon forms as two distinct horizons, which join at later v. In the limit $c \to 8^-$, this joining occurs at later and later v. At $c = 8$, these two horizons have joined. Note that despite the existence of horizons, choosing $c < 8$ implies that the square of the electric charge is negative.

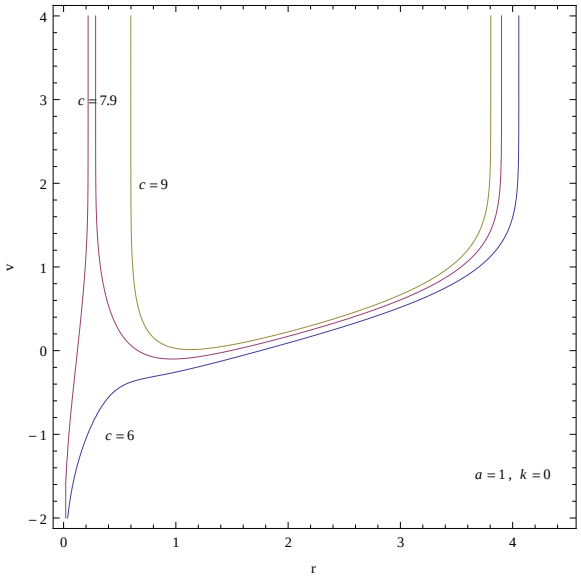

Figure 5.8: Apparent Horizons for the case $P = k\rho^a$, with $a = 1$, $k = 0$, and $C_1(v) = c\sqrt{\frac{\theta}{\pi}}m(v)$, and $m(v) \to 5\sqrt{\theta}$ as $v \to \infty$

Choosing $0 \leq a < 1$ restricts us to $k = 0$. We can see this by assuming $a \equiv \frac{n}{1+n}$, $n \in \mathbb{Z}$. We then have the dominant condition

$$\begin{aligned} \rho - k\rho^{\frac{n}{1+n}} &\geq 0 \\ \rho\left(1 - k\rho^{\frac{-1}{1+n}}\right) &\geq 0. \end{aligned} \tag{5.45}$$

The result is then

$$k\rho^{\frac{-1}{1+n}} \leq 1 \implies k \leq \rho^{\frac{1}{1+n}}. \tag{5.46}$$

Since ρ has a minimum of zero for either $m = 0$ or $r \to \infty$, then $k = 0$. The behaviour of this case has already been discussed.

If $a = 1$, then $P = k\rho$, and the dominant condition is then

$$(1 - k)\rho \geq 0. \tag{5.47}$$

Since $\rho \geq 0$ for all v and r, the parameter choice is limited to $k \leq 1$.

For $k = 1$, we have the rather simple

$$M(v, r) = -\frac{C_1(v)}{r} \tag{5.48}$$

which gives a metric function of

$$f(v, r) = 1 + \frac{2C_1(v)}{r^2}. \tag{5.49}$$

this appears to be a classical, but mass-less, charged Vaidya with $Q = \sqrt{2C_1(v)}$. While this is interesting, we may prefer to choose $C_1(v) = 0$ so that $a = k = 1$ gives Minkowski space.

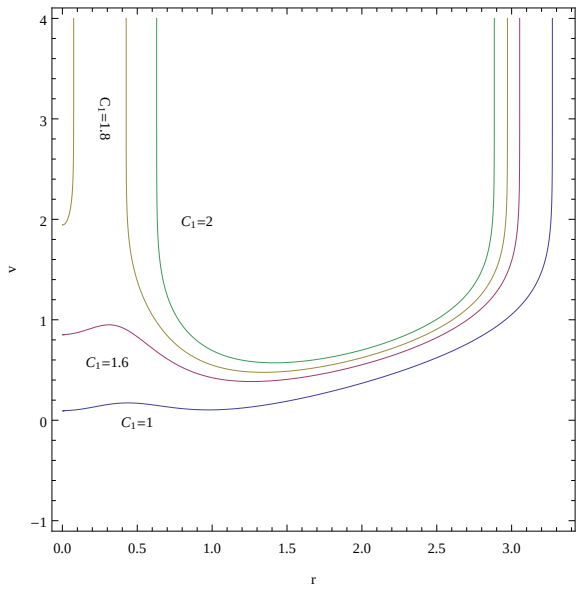

Figure 5.9: Apparent horizons for the case $P = k\rho^a$, with $a = 1$, $k = 0.2$ and $C_1(v)$ equal to the constants shown, and $m(v) \to 5\sqrt{\theta}$ as $v \to \infty$.

If $a = 1$, and $0 < k < 1$, then the restriction on $C_1(v)$ is similar to that of equation 5.44:

$$C_1(v) > (1-k) \cdot 8\sqrt{\frac{\theta}{\pi}} m(v). \tag{5.50}$$

The metric function reads

$$f(v,r) = 1 - \frac{4(1-k)\,\mathcal{E}\left(\frac{r}{2\sqrt{\theta}}\right) m(v)}{r} + \frac{2\left(8\sqrt{\frac{\theta}{\pi}}(k-1)\mathrm{e}^{-\frac{r^2}{4\theta}} m(v) + C_1(v)\right)}{r^2} \tag{5.51}$$

Plots of this function with $k = 0.2$, with various choices of $C_1(v)$, are found in Figure 5.9. Note that the number of horizons varies with $C_1(v)$.

Finally, for the choice $a \equiv 1 + \frac{1}{n} > 1$, $n \in \mathbb{Z}$, the value of k is restricted as

$$\begin{aligned} \rho - k\rho^{1+\frac{1}{n}} &\geq 0 \\ \rho\left(1 - k\rho^{\frac{1}{n}}\right) &\geq 0. \end{aligned} \tag{5.52}$$

Thus we have

$$k\rho^{\frac{1}{n}} \leq 1. \tag{5.53}$$

For example, choosing $a = 2$ $(n = 1)$ gives $k \leq \rho^{-1} \leq \rho_{\max}^{-1}$. Since we are choosing the mass function to be increasing to a maximum mass m_f as $v \to \infty$, we have specifically

$$k \leq \frac{(4\pi\theta)^{3/2}}{m_f}. \tag{5.54}$$

To further this example, we choose $m(v) = \frac{5\sqrt{\theta}}{2}(1 + \mathcal{E}(v))$, and $k = 0.25$, which satisfies the inequality above.

The metric function then reads

$$f(v,r) = 1 - \frac{2}{r}\left(2\,\mathcal{E}\left(\frac{r}{2\sqrt{\theta}}\right)m(v) - \frac{k\,\mathcal{E}\left(\frac{r}{\sqrt{2\theta}}\right)m^2(v)}{8\sqrt{2}\pi^{3/2}\theta^{3/2}}\right) \tag{5.55}$$

$$+ \frac{1}{r^2}\left(2C_1(v) + \frac{\mathrm{e}^{-\frac{r^2}{2\theta}}m(v)\left(km(v) - 32\mathrm{e}^{\frac{r^2}{4\theta}}\pi^{3/2}\theta^{3/2}\right)}{2\pi^2\theta}\right) \tag{5.56}$$

There are also restrictions on $C_1(v)$, which are

$$C_1(v) > \frac{m_f\left(32\pi^{3/2}\theta^{3/2} - km_f\right)}{4\pi^2\theta} \tag{5.57}$$

where $m(v) \to m_f$ as $v \to \infty$. Plots of this function for various choices of $C_1(v)$ are presented in Figure 5.10. For larger $C_1(v)$, the two horizons merge to an extremal-like state. Smaller values of $C_1(v)$ are not permitted by the bounding inequality above.

In the classical work by Husain, $k = \frac{1}{2}$ was a critical value that determined the asymptotic behaviour of the spacetime. This was due to the fact that k determined

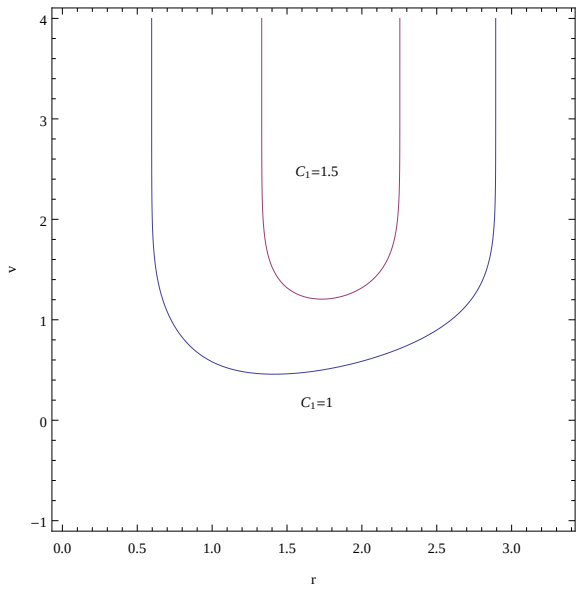

Figure 5.10: Apparent horizons for the case $P = k\rho^a$, with $a = 2$, $k = 0.25$ and $C_1(v)$ equal to the constants shown, and $m(v) \to 5\sqrt{\theta}$ as $v \to \infty$.

the powers of r in the metric function. Here, we have no such consequence; as such, k does not determine asymptoticity. In fact, for all k and a, the noncommutative spacetime with state $P = k\rho^a$ is asymptotically flat.

As was seen above, the usual noncommutative solutions rarely satisfy the energy conditions. As such, this form of a noncommutative spacetime may be preferable, as it was found with the requirement that the dominant energy condition be satisfied. Further topics to consider would include the radiative case, where M decreases, as per an evaporation process, and consequently its thermodynamic properties. These have already been extensively discussed (for example, [32, 48, 41, 4, 38, 39]), and a comparison is worthwhile. As well, another equation of state to consider is that of strange quark matter, where $P = \frac{1}{3}(\rho - 4B)$. This is similar to the state considered here, with $a = 1$, $k = 1/3$, but with an added constant. Lastly, one could also investigate lower- or higher-dimensional solutions with equivalent states.

Chapter 6

Conclusion

As a model of quantum gravity, the noncommutative theory reviewed here aims to transfer an uncertainty principle to the theory of gravity. Assuming a noncommutativity of spatial coordinates,

$$[x^\alpha, x^\beta] = \theta^{\alpha\beta}, \tag{6.1}$$

a "fuzziness" of space is created. This models the uncertainty principle, which precludes arbitrarily-high precision in measurement of spatial coordinates. This change in the geometry of space then modifies any metric. Under this approach, several solutions to the Einstein equations have been found, including analogues of the Schwarzschild, Reissner-Nordström and BTZ solutions, including other lower- and higher-dimensional solutions. Some time-dependent solutions have been found, in explicit t and r coordinates. The noncommutative solutions feature similar characteristic behaviours. With the inclusion of the noncommutative relation, a mass density function is created,

$$\rho(v, r) = \frac{M}{\sqrt{\pi} r} \mathrm{e}^{-\frac{r^2}{4\theta}}. \tag{6.2}$$

Mass is diffused over a region of $\sqrt{\theta}$, suggesting that $\sqrt{\theta}$ is the smallest observable area due to the uncertainty in spatial coordinates. Using this density function, the metric function that results is in terms of the lower incomplete gamma function,

$$\gamma(s,x) = \int_{t=0}^{x} t^{s-1}\mathrm{e}^{t}dt. \tag{6.3}$$

Of the resulting effects, foremost is a change in horizon behaviour. The noncommutativity adds an extra interior horizon, which is unstable. Classically, a larger mass parameter will extend (linearly) the outer horizon to larger r: in the Schwarzschild solution, $r = 2M$; in Reissner-Nordström, $r = M \pm \sqrt{M^2 - Q^2}$. The inner horizon shrinks with greater M, so that beyond a critical value, the inner horizon "disappears" inside $r = \sqrt{\theta}$, where this is assumed to be the smallest observable distance. There is a minimal mass, however, below which no horizon exists. At this minimal mass, there is a single horizon, and the black hole is called extremal.

In an analogous Reissner-Nordström case, two horizons still exist. We have shown that this is a problematic part of the solution. In a classical Reissner-Nordström solution, there are two horizons, both of which scale with M (and Q). One would expect that as M grows from very small (modelled by a noncommutative solution) to very large (transitioning to a classical solution) that the horizons would behave accordingly. This is not the case, and the noncommutative Reissner-Nordström solution behaves more like the Schwarzschild case, in that the horizons scale similarly with changes in M. At large M, the interior horizon disappears, and the outer horizon grows. Furthermore, the presence of the gamma functions in the Reissner-Nordström solution modifies the charge terms so that they contribute to mass. The charged portion of the metric function has two terms, one of which is proportional to r^{-2} and resembles the classical charge term, while there is an extra term proportional to r^{-1} which modifies the mass.

In this work we began with a noncommutative modification of the classical Vaidya solution, in the usual null (Eddington-Finkelstein) coordinates. We limited ourselves to ingoing coordinates and an increasing mass function, mimicking black hole formation. Our mass function was chosen with an initial mass of zero, so that the spacetime began with no black hole present. In this context, we considered two time-dependent noncommutative solutions: with and without charge.

In time-dependent noncommutative solution, there is a minimal mass at which the apparent horizon forms. At this point, there is a single horizon, and we have called this point extremal. While it is not possible to determine this point – a locus labelled (M, Q, r_H) – analytically, we aimed to find some relation between the three parameters of this point: M, Q, and r. Using numerical methods we solved a pair of equations to find this relation. The first used was the metric function which of course is zero on the horizon. The second is the equation describing the acceleration of a Killing vector. On the horizon, this equation is simply the surface gravity. Solving these two simultaneously, we were able to see the interaction between these three parameters at extremality.

Considering that charge is proportional to mass, $Q = \alpha M$, we found that as charge grows, the minimum mass necessary to form a black hole is less; this is understandable in light of the fact that the charge contributes to mass in a noncommutative Reissner-Nordström black hole. As well, the areal radius at extremality is also proportional to Q, though seemingly inversely-proportional to mass. In a classical spacetime, the extremal limit is that $Q \leq M$ necessarily. In a noncommutative spacetime, this restriction is not evident, and what would have been called "superextremal" is mathematically possible. As such, there is an "extremal limit" for the locus (M, Q, r_H): as Q/M grows, we attain a limit of $M \approx 0$, and $r_H \approx Q \approx 5\sqrt{\theta}$.

Using a generalized expansion of the stress-energy tensor, we were able to evaluate the time-dependent (and static) noncommutative solutions in light of the energy conditions. Violation of the energy conditions is at times acceptable, provided there is a good physical reason to believe it is acceptable. These allowable violations may include regions close to the singularity, Hawking radiation, and cosmological solutions. Unacceptable violations may be global in nature, or large-regions in "regular space". In a noncommutative context, where all regions are considered "small", violations may or may not be acceptable. Given that observations outside a noncommutative black hole are theoretically possible with sufficient technological advance, one could consider these violations to be unacceptable.

The stress-energy tensor used herein considers two possible matter fields. Using two cross-normalized vectors normal to cross-sections of the horizon, ℓ^α and n^α, the tensor is split into two parts,

$$T_{\alpha\beta} = T^{(m)}_{\alpha\beta} + T^{(n)}_{\alpha\beta} \tag{6.4}$$

where

$$T^{(m)}_{\alpha\beta} = \mu \ell_\alpha \ell_\beta$$

$$T^{(n)}_{\alpha\beta} = (\rho + P)\left(\ell_\alpha n_\beta + \ell_\beta n_\alpha\right) + P g_{\alpha\beta}$$

Under this expansion, violations of the energy tensor are easily classifiable, and we have seen that violations occur for non-trivial intervals of r. The noncommutative Schwarzschild solution, for example, requires that $r \geq 2\sqrt{\theta}$; the dominant condition requires $2\sqrt{\theta} \leq r \leq \sqrt{8\theta}$. Under the dominant condition, it is easily possible to choose a mass parameter sufficiently small so that there is violation outside the black hole, but not inside. The cause of these violations is the heavy dependence on r in the metric function. Because we have chosen a gaussian distribution for matter

density, the stress-energy tensor has components that vary with r. In our discussion, we showed that such quantities as density and pressure vary greatly over r, and do not easily satisfy the energy conditions.

As a remedy to these violations, we imposed an equation of state that is similar to polytropic fluids, where

$$P = k\rho^a. \tag{6.5}$$

Generally, polytropic fluids model such objects as neutron stars, and feature different objects for differing values of $a > 1$. In this work, as in a previous, commutative, work by V Husain, we consider $a \leq 1$ as well. Using this assumption, and a time-dependent metric in ingoing null coordinates, we derive an alternate noncommutative solution that satisfies the dominant energy condition.

This solution bears resemblance to current noncommutative solutions, but also adds new time-dependent parameters. These parameters can be chosen to create varying solutions. It is possible to create Minkowski space ($P = \rho$), a massless-but-charged black hole (also $P = \rho$), and a Reissner-Nordström-like solution. Furthermore, fine-tuning these parameters will have distinct effects on the nature of the final solution. One choice of these parameters will create a charged black hole with three horizons: two outer horizons that begin at extremality (i.e., a single horizon), and an inner horizon. This is a welcome result, in that it shows what we would expect from a noncommutative Reissner-Nordström solution: an inner noncommutative horizon (as is present in a Schwarzschild solution), and two outer, "classical", horizons. However, the behaviour of this inner horizon is opposite to our expectations: it grows proportionally to the mass and charge parameters. In all cases, this solution is asymptotically flat, which differs from the results found by Husain.

Following this set of results, it would be worthwhile to consider the reverse, the

outgoing-coordinate/decreasing-mass case, and its thermodynamic properties. While most noncommutative works choose to use an anisotropic matter model, there are other fluids worth considering. Foremost would be strange quark matter, which is likely relevant to the study of the cosmological production of early black holes. This fluid source is defined by $P = \frac{1}{3}(\rho - 4B)$. The addition of this constant makes the problem much more difficult; a perturbative method with B chosen to be small may be a fruitful approach.

Chapter 7

Appendix

We demonstrate here a solution of the Einstein equations for a spherically-symmetric, time-dependent, noncommutative spacetime with electric charge. This is the noncommutative-analogous solution to the Reissner-Nordström solution. A similar process can be carried out for a noncommutative Schwarzschild solution. This process is available in many sources, including [37] for the noncommutative Schwarzschild case, and [4] for the noncommutative Reissner-Nordström case.

The current density is

$$J^{\alpha} = \rho_{\mathrm{el}}(v, r)\delta_0^{\alpha} \tag{7.1}$$

where

$$\rho_{\mathrm{el}}(v, r) = \frac{Q(v)}{(4\pi\theta^{3/2})}\mathrm{e}^{-\frac{r^2}{4\theta}}. \tag{7.2}$$

The equations describing this charge are the electromagnetic tensor

$$F^{\alpha\beta} = \delta^{0[\alpha|}\delta^{r|\beta]}E(v, r) \tag{7.3}$$

and the Maxwell equation

$$\frac{1}{\sqrt{-g}}\partial_\alpha\left(\sqrt{-g}F^{\alpha\beta}\right) = J^\beta \tag{7.4}$$

where $E(v,r)$ is the electric field.

We presume that the spacetime is spherically symmetric, so that

$$g_{\alpha\beta} = \begin{pmatrix} -f(v,r) & 1 & 0 & 0 \\ 1 & 0 & 0 & 0 \\ 0 & 0 & r^2 & 0 \\ 0 & 0 & 0 & r^2\sin^2\vartheta \end{pmatrix}. \tag{7.5}$$

From (7.3) we have $-F^{vr} = F^{rv} = E(v,r)$, and $F^{\alpha\beta} = 0$ otherwise. From (7.5), $\sqrt{-g} = r^2$.

Solving the Maxwell equation (7.4) with the charge density (7.2), we have the equation

$$\frac{1}{r^2}\partial_r\left(r^2E(v,r)\right) = \frac{Q(v)}{(4\pi\theta^{3/2})}\mathrm{e}^{-\frac{r^2}{4\theta}}. \tag{7.6}$$

The solution to the electric field is

$$E(v,r) = \frac{Q(v)}{2\pi r^2}\gamma\left(\frac{3}{2},\frac{r^2}{4\theta}\right). \tag{7.7}$$

The electromagnetic stress-energy tensor is of the form

$${}_{\mathrm{el}}T_{\alpha\beta} = \frac{1}{4\pi}\left(F_{\alpha\mu}F^{\mu}_{\beta} + \frac{1}{4}g_{\alpha\beta}F^{\mu\nu}F_{\mu\nu}\right) \tag{7.8}$$

which evaluates to

$$ {}_{\text{el}}T_{\alpha\beta} = \frac{E^2(v,r)}{8\pi} g_{\alpha\beta}. \tag{7.9} $$

The matter-component of the stress-energy tensor – based on the form of metric chosen – reads

$$ {}_{\text{matt}}T_{\alpha}{}^{\beta} = \begin{pmatrix} T_t{}^t & T_t{}^r & 0 & 0 \\ T_r{}^t & T_r{}^r & 0 & 0 \\ 0 & 0 & T_\vartheta{}^\vartheta & 0 \\ 0 & 0 & 0 & T_\phi{}^\phi \end{pmatrix}. \tag{7.10} $$

To determine $f(v,r)$, the only unknown portion of the metric, we solve

$$ G^t{}_t = 8\pi \left({}_{\text{matt}}T^t{}_t + {}_{\text{el}}T^t{}_t \right). \tag{7.11} $$

This gives the PDE

$$ -\frac{1}{r^2} - 8\pi T_r{}^r + \frac{f + r(rE^2(v,r) + \partial_r f)}{r^2} = 0 \tag{7.12} $$

which can be reworked to the form

$$ 8\pi r^2 T_r{}^r - E^2(v,r) = -\partial_r(r(1-f)). \tag{7.13} $$

Integrating, we obtain

$$ f(v,r) = 1 + \frac{1}{r} \int \left(8\pi r^2 T_r{}^r - E^2(v,r) \right) \mathrm{d}r. \tag{7.14} $$

With $T_r{}^r = \rho_{\rm matt}(v,r) = \frac{M(v)}{(4\pi\theta^{3/2})}\gamma\left(\frac{3}{2},\frac{r^2}{4\theta}\right)$, we find then

$$f(v,r) = 1 - \frac{4M(v)}{\sqrt{\pi}r^2}\gamma\left(\frac{3}{2},\frac{r^2}{4\theta}\right) + \frac{Q^2(v)}{\pi r^2}\left(\gamma\left(\frac{1}{2},\frac{r^2}{4\theta}\right)^2 - \frac{r}{\sqrt{2\theta}}\gamma\left(\frac{1}{2},\frac{r^2}{2\theta}\right)\right) \qquad (7.15)$$

Bibliography

[1] Comments on and Comments on Comments on Verlinde's paper "On the Origin of Gravity and the Laws of Newton". 2010. URL http://arxiv.org/abs/1003.1015.

[2] The Nobel Prize in Physics 1921, April 2013. URL http://www.nobelprize.org/nobel_prizes/physics/laureates/1921/.

[3] Solvay Conference, April 2013. URL http://en.wikipedia.org/wiki/Solvay_Conference.

[4] Stefano Ansoldi, Piero Nicolini, Anais Smailagic, and Euro Spallucci. Noncommutative geometry inspired charged black holes. *Physics Letters B*, 645(2-3): 261–266, December 2006. ISSN 03702693. doi: 10.1016/j.physletb.2006.12.020. URL http://dx.doi.org/10.1016/j.physletb.2006.12.020.

[5] Nima Arkani-Hamed, Jacob L. Bourjaily, Freddy Cachazo, Alexander B. Goncharov, Alexander Postnikov, and Jaroslav Trnka. Scattering Amplitudes and the Positive Grassmannian, December 2012. URL http://arxiv.org/abs/1212.5605.

[6] Abhay Ashtekar. New Variables for Classical and Quantum Gravity. *Physical*

Review Letters, 57(18):2244–2247, November 1986. doi: 10.1103/physrevlett.57.2244. URL http://dx.doi.org/10.1103/physrevlett.57.2244.

[7] Rabin Banerjee, Sunandan Gangopadhyay, and Sujoy K. Modak. Voros product, Noncommutative Schwarzschild Black Hole and Corrected Area Law. *Physics Letters B*, 686(2-3):181–187, February 2010. ISSN 03702693. doi: 10.1016/j.physletb.2010.02.034. URL http://dx.doi.org/10.1016/j.physletb.2010.02.034.

[8] Prasad Basu, Biswajit Chakraborty, and Frederik G. Scholtz. A unifying perspective on the Moyal and Voros products and their physical meanings. *Journal of Physics A: Mathematical and Theoretical*, 44(28):285204+, January 2011. ISSN 1751-8113. doi: 10.1088/1751-8113/44/28/285204. URL http://dx.doi.org/10.1088/1751-8113/44/28/285204.

[9] Ivan Booth and Stephen Fairhurst. Extremality conditions for isolated and dynamical horizons. *Physical Review D*, 77(8), April 2008. ISSN 1550-7998. doi: 10.1103/physrevd.77.084005. URL http://dx.doi.org/10.1103/physrevd.77.084005.

[10] Eric Brown and Robert B. Mann. Instability of the Noncommutative Geometry Inspired Black Hole, December 2010. URL http://arxiv.org/abs/1012.4787.

[11] M. Chaichian, A. Tureanu, R. B. Zhang, and X. Zhang. Riemannian Geometry of Noncommutative Surfaces. *Journal of Mathematical Physics*, 49(7):073511+, July 2008. ISSN 00222488. doi: 10.1063/1.2953461. URL http://dx.doi.org/10.1063/1.2953461.

[12] Ali H. Chamseddine. Deforming Einstein's Gravity. *Physics Letters B*, 504(1-2):

33–37, September 2000. ISSN 03702693. doi: 10.1016/s0370-2693(01)00272-6. URL http://dx.doi.org/10.1016/s0370-2693(01)00272-6.

[13] Sergio Doplicher, Klaus Fredenhagen, and John E. Roberts. The quantum structure of spacetime at the Planck scale and quantum fields, March 2003. URL http://arxiv.org/abs/hep-th/0303037.

[14] Albert Einstein. Die Feldgleichungen der Gravitation. In *Preussische Akademie der Wissenschaften, Sitzungsberichte*, pages 844–847, 1915.

[15] Rodolfo Gambini and Jorge Pullin. *A First Course in Loop Quantum Gravity*. Oxford University Press, Great Clarendon Street, Oxford, OX2 6DP, 2011. ISBN 978-0-19-959075-9.

[16] Sunandan Gangopadhyay. Noncommutative inspired Schwarzschild black hole, Voros product and Komar energy, December 2012. URL http://arxiv.org/abs/1212.4049.

[17] Roy J. Glauber. Coherent and Incoherent States of the Radiation Field. *Physical Review Online Archive (Prola)*, 131(6):2766–2788, September 1963. doi: 10.1103/physrev.131.2766. URL http://dx.doi.org/10.1103/physrev.131.2766.

[18] Jaume Gomis and Thomas Mehen. Space-Time Noncommutative Field Theories And Unitarity. *Nuclear Physics B*, 591(1-2):265–276, August 2000. ISSN 05503213. doi: 10.1016/s0550-3213(00)00525-3. URL http://dx.doi.org/10.1016/s0550-3213(00)00525-3.

[19] Jerry B. Griffiths and Jiří Podolský. *Exact Space-Times in Einstein's General Relativity*. Cambridge University Press, 2009.

[20] Razvan Gurau. *La rénormalisation dans la théorie non commutative des champs*. PhD thesis, Université Paris 11, 2007. URL http://arxiv.org/abs/0802.0940.

[21] T. Harko and K. S. Cheng. Collapsing strange quark matter in Vaidya geometry. *Physics Letters A*, 266(4-6):249–253, April 2001. ISSN 03759601. doi: 10.1016/s0375-9601(00)00005-0. URL http://dx.doi.org/10.1016/s0375-9601(00)00005-0.

[22] James B. Hartle. *Gravity: An Introduction to Einstein's General Relativity*. Addison Wesley, 2003.

[23] Viqar Husain. Exact solutions for null fluid collapse. *Physical Review D*, 53(4): R1759–R1762, November 1995. ISSN 0556-2821. doi: 10.1103/physrevd.53.r1759. URL http://dx.doi.org/10.1103/physrevd.53.r1759.

[24] Archil Kobakhidze. Noncommutative corrections to classical black holes. *Physical Review D*, 79(4), December 2007. ISSN 1550-7998. doi: 10.1103/physrevd.79.047701. URL http://dx.doi.org/10.1103/physrevd.79.047701.

[25] Maxim Kontsevich. Deformation quantization of Poisson manifolds, I. *Letters in Mathematical Physics*, 66(3):157–216, September 1997. ISSN 0377-9017. doi: 10.1023/b:math.0000027508.00421.bf. URL http://dx.doi.org/10.1023/b:math.0000027508.00421.bf.

[26] Alexis Larranaga and Juan M. Tejeiro. Three Dimensional Charged Black Hole Inspired by Noncommutative Geometry, April 2010. URL http://arxiv.org/abs/1004.1608.

[27] Robert B. Mann and Piero Nicolini. Cosmological production of noncommutative black holes. *Physical Review D*, 84(6), September 2011. ISSN 1550-

7998. doi: 10.1103/physrevd.84.064014. URL http://dx.doi.org/10.1103/physrevd.84.064014.

[28] S. Hamid Mehdipour. Hawking radiation as tunneling from a Vaidya black hole in noncommutative gravity. *Physical Review D*, 81(12), June 2010. ISSN 1550-7998. doi: 10.1103/physrevd.81.124049. URL http://dx.doi.org/10.1103/physrevd.81.124049.

[29] S. Hamid Mehdipour. Gravitational energy of a noncommutative Vaidya black hole. *Canadian Journal of Physics*, 91(3):242–245, December 2012. ISSN 0008-4204. doi: 10.1139/cjp-2012-0485. URL http://dx.doi.org/10.1139/cjp-2012-0485.

[30] Leonardo Modesto, John W. Moffat, and Piero Nicolini. Black holes in an ultraviolet complete quantum gravity. *Physics Letters B*, 695(1-4):397–400, December 2010. ISSN 03702693. doi: 10.1016/j.physletb.2010.11.046. URL http://dx.doi.org/10.1016/j.physletb.2010.11.046.

[31] J. E. Moyal. Quantum mechanics as a statistical theory. *Mathematical Proceedings of the Cambridge Philosophical Society*, 45(01):99–124, January 1949. ISSN 1469-8064. doi: 10.1017/s0305004100000487. URL http://dx.doi.org/10.1017/s0305004100000487.

[32] Yun S. Myung, Yong-Wan Kim, and Young-Jai Park. Thermodynamics and evaporation of the noncommutative black hole. *Journal of High Energy Physics*, 2007(02):012, January 2007. ISSN 1029-8479. doi: 10.1088/1126-6708/2007/02/012. URL http://dx.doi.org/10.1088/1126-6708/2007/02/012.

[33] Piero Nicolini. A model of radiating black hole in noncommutative geometry. *Journal of Physics A: Mathematical and General*, 38(39):L631–L638, July 2005.

ISSN 0305-4470. doi: 10.1088/0305-4470/38/39/l02. URL http://dx.doi.org/10.1088/0305-4470/38/39/l02.

[34] Piero Nicolini. Noncommutative Black Holes, The Final Appeal To Quantum Gravity: A Review, February 2009. URL http://arxiv.org/abs/0807.1939.

[35] Piero Nicolini and Euro Spallucci. Noncommutative geometry inspired dirty black holes. *Classical and Quantum Gravity*, 27(1):015010+, November 2009. ISSN 0264-9381. doi: 10.1088/0264-9381/27/1/015010. URL http://dx.doi.org/10.1088/0264-9381/27/1/015010.

[36] Piero Nicolini and Elizabeth Winstanley. Hawking emission from quantum gravity black holes, November 2011. URL http://arxiv.org/abs/1108.4419.

[37] Piero Nicolini, Anais Smailagic, and Euro Spallucci. Noncommutative geometry inspired Schwarzschild black hole. *Physics Letters B*, 632(4):547–551, November 2005. ISSN 03702693. doi: 10.1016/j.physletb.2005.11.004. URL http://dx.doi.org/10.1016/j.physletb.2005.11.004.

[38] Kourosh Nozari and Sara Islamzadeh. Tunneling of massive and charged particles from noncommutative reissner-nordström black hole, July 2012. URL http://arxiv.org/abs/1207.1177.

[39] Kourosh Nozari and S. Hamid Mehdipour. Noncommutative Inspired Reissner-Nordström Black Holes in Large Extra Dimensions. *Communications in Theoretical Physics*, 53(3):503–513, June 2009. ISSN 0253-6102. doi: 10.1088/0253-6102/53/3/20. URL http://dx.doi.org/10.1088/0253-6102/53/3/20.

[40] Eric Poisson. *A Relativist's Toolkit: The Mathematics of Black-Hole Mechanics*. Cambridge University Press, 2004.

[41] Farook Rahaman, P. K. F. Kuhfittig, B. C. Bhui, Masiur Rahaman, Saibal Ray, and U. F. Mondal. BTZ black holes inspired by noncommutative geometry, March 2013. URL http://arxiv.org/abs/1301.4217.

[42] C. Rovelli. Ashtekar formulation of general relativity and loop-space nonperturbative quantum gravity: a report. *Classical and Quantum Gravity*, 8(9):1613–1676, September 1991. ISSN 0264-9381. doi: 10.1088/0264-9381/8/9/002. URL http://dx.doi.org/10.1088/0264-9381/8/9/002.

[43] Carlo Rovelli and Lee Smolin. Loop space representation of quantum general relativity. *Nuclear Physics B*, 331(1):80–152, February 1990. ISSN 05503213. doi: 10.1016/0550-3213(90)90019-a. URL http://dx.doi.org/10.1016/0550-3213(90)90019-a.

[44] F. G. Scholtz, L. Gouba, A. Hafver, and C. M. Rohwer. Formulation, Interpretation and Application of non-Commutative Quantum Mechanics. *Journal of Physics A: Mathematical and Theoretical*, 42(17):175303+, December 2008. ISSN 1751-8113. doi: 10.1088/1751-8113/42/17/175303. URL http://dx.doi.org/10.1088/1751-8113/42/17/175303.

[45] M. Sharif and G. Abbas. Singularities of Noncompact Charged Objects. *Chinese Physics B*, 22(3):030401+, February 2013. ISSN 1674-1056. doi: 10.1088/1674-1056/22/3/030401. URL http://dx.doi.org/10.1088/1674-1056/22/3/030401.

[46] Anais Smailagic and Euro Spallucci. UV divergence-free QFT on noncommutative plane. *Journal of Physics A: Mathematical and General*, 36(39):L517–L521, August 2003. ISSN 0305-4470. doi: 10.1088/0305-4470/36/39/103. URL http://dx.doi.org/10.1088/0305-4470/36/39/103.

[47] Anais Smailagic and Euro Spallucci. Lorentz invariance and unitarity in UV finite NCQFT, June 2004. URL http://arxiv.org/abs/hep-th/0406174.

[48] Euro Spallucci, Anais Smailagic, and Piero Nicolini. Non-commutative geometry inspired higher-dimensional charged, black holes. *Physics Letters B*, 670(4-5): 449–454, November 2008. ISSN 03702693. doi: 10.1016/j.physletb.2008.11.030. URL http://dx.doi.org/10.1016/j.physletb.2008.11.030.

[49] Erik Verlinde. On the origin of gravity and the laws of Newton. *Journal of High Energy Physics*, 2011(4):1–27, 2011. doi: 10.1007/JHEP04(2011)029. URL http://dx.doi.org/10.1007/JHEP04\%282011\%29029.

[50] Robert M. Wald. *General Relativity*. University of Chicago Press, 1984.

[51] Anzhong Wong and Yumei Wu. Generalized Vaidya Solutions. *General Relativity and Gravitation*, 31:107–114, 1999.

[52] R. B. Zhang and Xiao Zhang. A noncommutative geometric approach to the quantum structure of spacetime, August 2011. URL http://arxiv.org/abs/1108.0249.